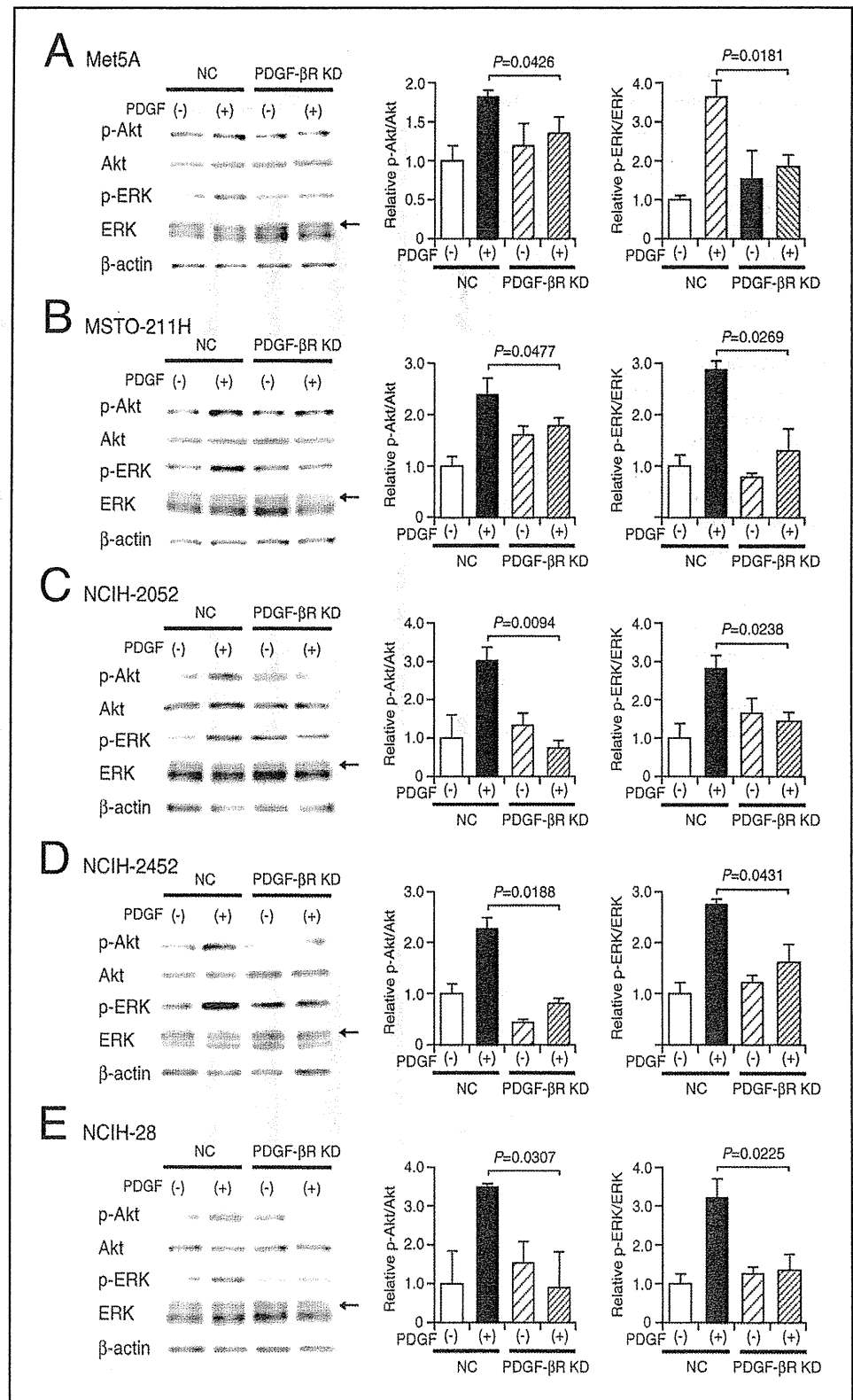


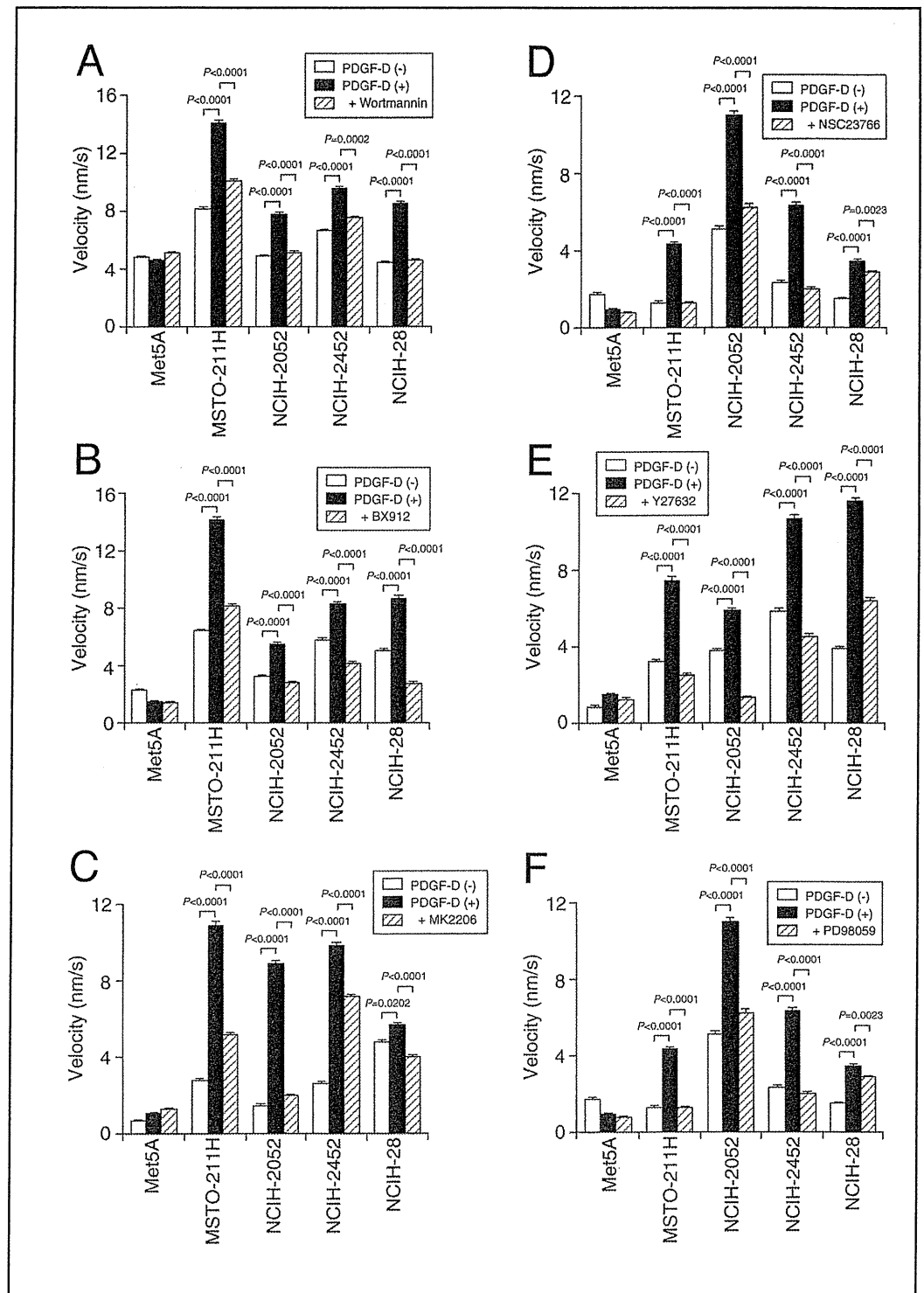
Fig. 5. PDGF-D-induced activation of Akt and ERK in mesothelioma cells. Western blotting was carried out in Met5A (A), MSTO-211H (B), NCIH-H2052 (C), NCIH-H2452 (D), and NCIH-28 cells (E), transfected with the NC siRNA (NC) or the PDGF- β R siRNA (PDGF- β R KD) before and after 10-min treatment with PDGF-D (40 ng/ml). In the blotting membranes shown, arrows indicate 44 kDa of ERK, corresponding to ERK1. In the graphs, expression levels for each protein were normalized by β -actin. Each value represents the mean (\pm SEM) ratio of phosphorylated Akt (p-Akt) against total amount of Akt or the phosphorylated ERK (p-ERK) against total amount of ERK ($n=4$ independent experiments). Note that each value before treatment with PDGF-D is regarded as 1. *P* values, Dunnett's test.



the Akt inhibitor MK2206, while Met5A cell migration was not affected by PDGF-D in the presence and absence of MK2206 (Fig. 6C). This indicates the participation of

Akt, a downstream effector of PDK1, in PDGF-D-engaged regulation of malignant mesothelioma cell chemotaxis.

Fig. 6. PDGF-D-induced facilitation of malignant mesothelioma cell chemotaxis through a PDGF- β receptor signaling pathway along a PI3 kinase/PDK1/Akt/Rac1/ROCK axis or by activating ERK1. Chemotaxis assay was carried out in cells as indicated by applying PDGF-D (4 ng) in the presence and absence of wortmanin (50 nmol)(A), BX912 (10 nmol)(B), MK2206 (5 nmol)(C), NSC23766 (100 nmol)(D), Y27632 (10 nmol)(E) or PD98059 (1 pmol) (F). In the graph, each value represents the mean (\pm SEM) velocity ($n=15$ independent experiments). P values, unpaired t -test.



PDGF-D-induced facilitation of malignant mesothelioma cell migration was significantly attenuated by the Rac1 inhibitor NSC23766, while Met5A cell migration was not affected by PDGF-D in the presence and absence of NSC23766 (Fig. 6D). This indicates the

participation of Rac1, a downstream effector of Akt, in PDGF-D-engaged regulation of malignant mesothelioma cell chemotaxis.

PDGF-D-induced facilitation of malignant mesothelioma cell migration was significantly suppressed

by the ROCK inhibitor Y27632, while Met5A cell migration was not affected by PDGF-D in the presence and absence of Y27632 (Fig. 6E). This indicates the participation of ROCK, a downstream effector of Rac1, in PDGF-D-engaged regulation of malignant mesothelioma cell chemotaxis.

PDGF-D-induced facilitation of malignant mesothelioma cell migration, alternatively, was significantly suppressed by the MEK1 inhibitor PD98059, while Met5A cell migration was not affected by PDGF-D in the presence and absence of PD98059 (Fig. 6F). This indicates that ERK1 still participates in PDGF-D-engaged regulation of malignant mesothelioma cell chemotaxis.

Overall, these results lead to a conclusion that PDGF-D promotes malignant mesothelioma cell chemotaxis as mediated via PDGF- $\beta\beta$ receptors linked to activation of PI3 kinase/PDK1/Akt/ Rac1/ROCK and ERK1.

Discussion

Chemotaxis, cell motility directed towards higher concentrations of chemoattractants, plays a critical role in invasion and metastasis of cancers [25]. The motility is regulated according to gradients of chemoattractants such as chemokines and growth factors, that activate chemokine receptors and receptor tyrosine kinases, respectively. Malignant mesothelioma cells are recognized to progressively invade into the peritoneum or the pleura. Several avenues of studies have suggested the implication of PDGF, a growth factor, in metastasis of a variety of cancers, but little is known about the effect on malignant mesothelioma cells.

In our earlier study, FBS facilitated malignant mesothelioma cell migration and the effect was inhibited by the uPA inhibitor UTI [24]. This suggests that FBS stimulates secretion of PDGF-D, that is converted to active dimer of PDGF-DD through uPA-mediated proteolytic processing, thereby activating PDGF- $\beta\beta$ receptors bearing facilitation of malignant mesothelioma cell chemotaxis. In the present study, FBS significantly increased the amount of extracellular PDGF-D for malignant mesothelioma cells such as MSTO-211H, NCIH-2052, NCIH-2452, and NCIH-28 cells. FBS also increased the amount of extracellular PDGF-D for non-malignant Met5A cells, but not significantly. This provides evidence for FBS-induced PDGF-D secretion from mesothelioma cells, with the extent being greater for malignant mesothelioma cells than that for non-malignant

mesothelioma cells. This also suggests that malignant mesothelioma cells favor an autocrine activation of PDGF- $\beta\beta$ receptors.

PDGF- $\beta\beta$ receptor is a receptor tyrosine kinase. For a PDGF- $\beta\beta$ receptor signaling pathway, activation of PDGF- $\beta\beta$ receptor by PDGF-D, i.e., activation of tyrosine kinase, phosphorylates insulin substrate protein (IRS)-1/-2. Phosphorylated IRS-1/-2, in turn, recruits and activates PI3 kinase, to produce phosphatidylinositol (3,4,5)-trisphosphate [PI (3,4,5) P_3] from phosphatidylinositol (4,5)-biphosphate [PI (4,5) P_2]. PI (3,4,5) P_3 binds to and activates PDK1, which phosphorylates and activates Akt. Activated Akt activates the small G-protein Rac1/Cdc42 followed by activation of the effector ROCK. For another PDGF- $\beta\beta$ receptor signaling pathway, activation of PDGF- $\beta\beta$ receptor by PDGF-D phosphorylates Shc2, to recruit and associate Grb2 and SOS, a guanine nucleotide exchange factor for Ras, thereby activating Ras. Activated Ras activates Raf, a serine/threonine protein kinase. Activated Raf phosphorylates and activates MEKK, a serine/threonine protein kinase, followed by phosphorylation and activation of MEK, a serine/threonine protein kinase, to phosphorylate and activate MAPK, a serine/threonine protein kinase. In the present study, PDGF-D increased phosphorylated Akt, i.e., the active form of Akt, and phosphorylated ERK1, the active form of ERK1, in all the non-malignant and malignant mesothelioma cells used here, and those effects were inhibited by knocking-down PDGF- $\beta\beta$ receptor. This suggests that PDGF- $\beta\beta$ receptor is capable of activating ROCK along a PI3 kinase/PDK1/Akt/Rac1 (Cdc42) axis and activating MAPK along a Ras/Raf/MEKK/MEK axis.

In the chemotactic assay, PDGF-D facilitated migration of all the malignant mesothelioma cells used here, MSTO-211H, NCIH-2052, NCIH-2452, and NCIH-28 cells, with the potency varying among cell types, while the facilitatory effect was not obtained with non-malignant Met5A cells. This confirms that PDGF-D serves as a chemoattractant for malignant mesothelioma cell chemotaxis. If this is true, then PDGF-D might facilitate malignant mesothelioma cell chemotaxis by activating PDGF- $\beta\beta$ receptors. PDGF-D-induced facilitation of malignant mesothelioma cell migration was abolished by knocking-down PDGF- $\beta\beta$ receptor, providing direct evidence for the implication of PDGF- $\beta\beta$ receptor in the facilitatory action of PDGF-D on malignant mesothelioma cell chemotaxis.

PDGF-D-induced facilitation of malignant mesothelioma cell migration was clearly prevented by the

PI3 kinase inhibitor wortmannin, the PDK1 inhibitor BX912, the Akt inhibitor MK2206, the Rac1 inhibitor NSC23766, or the ROCK inhibitor Y27632. This indicates that PDGF-D promotes malignant mesothelioma cell chemotaxis through a PDGF- $\beta\beta$ receptor signaling pathway along a PI3 kinase/PDK1/Akt/Rac1/ROCK axis. PDGF-D-induced facilitation of malignant mesothelioma cell migration, on the other hand, was still inhibited by the MEK1 inhibitor PD98059, suggesting that PDGF-D promotes malignant mesothelioma cell chemotaxis through another PDGF- $\beta\beta$ receptor signaling pathway along a Ras/Raf/MEKK/MEK/MAPK axis.

Several avenues of studies have provided direct and indirect evidence for PDGF-D/PDGF- $\beta\beta$ receptor as a mediator for development, progression, and metastasis in a variety of cancer cells [15-23]. Imatinib mesylate, an inhibitor of receptors tyrosine kinases including PDGF- $\beta\beta$ receptor, has been attempted for treatment of malignant

mesothelioma as well as other cancers. Unfortunately, clinical trials with imatinib mesylate show limited efficacy in malignant mesothelioma, while the drug induces cytotoxicity and apoptosis selectively on PDGF- $\beta\beta$ receptor-positive mesothelioma cells [26-28]. The results presented here point to the critical role of PDGF-D/PDGF- $\beta\beta$ receptor in malignant mesothelioma cell chemotaxis. This may represent the mechanism underlying rapid and aggressive invasion of malignant mesothelioma cells into the peritoneum or the pleura. PDGF-D/PDGF- $\beta\beta$ signaling cascades, accordingly, could be a promising target of malignant mesothelioma therapy, even though imatinib mesylate currently exhibits less beneficial effect in clinical trials.

In conclusion, the results of the present study show that PDGF-D activates PDGF- $\beta\beta$ receptors in an autocrine manner, involving activation of PI3 kinase/PDK1/Akt/Rac1/ROCK and MAPK, to promote malignant mesothelioma cell chemotaxis.

References

- Nakano T: Malignant mesothelioma-diagnosis and treatment strategies. *Gan To Kagaku Ryoho* 2006;33:1215-1220.
- Garlepp MJ, Leong CC: Biological and immunological aspects of malignant mesothelioma. *Eur Respir J* 1995;8:643-650.
- Upham JW, Garlepp MJ, Musk AW, Robinson BW: Malignant mesothelioma: new insights into tumour biology and immunology as a basis for new treatment approaches. *Thorax* 1995;50:887-893.
- Halper J: Growth factors as active participants in carcinogenesis: a perspective. *Vet Pathol* 2010;47:77-97.
- Filiberti R, Marroni P, Neri M, Ardizzoni A, Betta PG, Cafferata MA, Canessa PA, Puntoni R, Ivaldi GP, Paganuzzi M: Serum PDGF-AB in pleural mesothelioma. *Tumour Biol* 2005;26:221-226.
- Versnel MA, Hagemeyer A, Bouts MJ, van der Kwast TH, Hoogsteden HC: Expression of *c-sis* (PDGF B-chain) and PDGF A-chain genes in ten human malignant mesothelioma cell lines derived from primary and metastatic tumors. *Oncogene* 1988;2:601-605.
- Gerwin BI, Lechner JF, Reddel RR, Roberts AB, Robbins KC, Gabrielson EW, Harris CC: Comparison of production of transforming growth factor- β and platelet-derived growth factor by normal human mesothelial cells and mesothelioma cell lines. *Cancer Res* 1987;47:6180-6184.
- Van der Meeren A, Seddon MB, Betsholtz CA, Lechner JF, Gerwin BI: Tumorigenic conversion of human mesothelial cells as a consequence of platelet-derived growth factor-A chain overexpression. *Am J Respir Cell Mol Biol* 1993;8:214-221.
- Metheny-Barlow LJ, Flynn B, van Gijssel HE, Marrogi A, Gerwin BI: Paradoxical effects of platelet-derived growth factor-A overexpression in malignant mesothelioma. Antiproliferative effects in vitro and tumorigenic stimulation in vivo. *Am J Respir Cell Mol Biol* 2001;24:694-702.
- Klominek J, Baskin B, Hauzenberger D: Platelet-derived growth factor (PDGF) BB acts as a chemoattractant for human malignant mesothelioma cells via PDGF receptor β -integrin $\alpha 3\beta 1$ interaction. *Clin Exp Metastasis* 1998;16:529-539.
- Zhong J, Gencay MM, Bubendorf L, Burgess JK, Parson H, Robinson BW, Tamm M, Black JL, Roth M: ERK1/2 and p38 MAP kinase control MMP-2, MT1-MMP, and TIMP action and affect cell migration: a comparison between mesothelioma and mesothelial cells. *J Cell Physiol* 2006;207:540-552.
- Alvarez RH, Kantarjian HM, Cortes JE: Biology of platelet-derived growth factor and its involvement in disease. *Mayo Clin Proc* 2006;81:1241-1257.
- Bergsten E, Uutela M, Li X, Pietras K, Ostman A, Heldin CH, Alitalo K, Eriksson U: PDGF-D is a specific, protease-activated ligand for the PDGF β -receptor. *Nat Cell Biol* 2001;3:512-516.

- 14 Fredriksson L, Ehnman M, Fieber C, Eriksson U: Structural requirements for activation of latent platelet-derived growth factor CC by tissue plasminogen activator. *J Biol Chem* 2005;280:26856-26862.
- 15 Wang Z, Ahmad A, Li Y, Kong D, Azmi AS, Banerjee S, Sarkar FH: Emerging roles of PDGF-D signaling pathway in tumor development and progression. *Biochim Biophys Acta* 2010;1806:122-130.
- 16 Ustach CV, Taube ME, Hurst NJ Jr, Bhagat S, Bonfil RD, Cher ML, Schuger L, Kim HR: A potential oncogenic activity of platelet-derived growth factor D in prostate cancer progression. *Cancer Res* 2004;64:1722-1729.
- 17 Ustach CV, Kim HR: Platelet-derived growth factor D is activated by urokinase plasminogen activator in prostate carcinoma cells. *Mol Cell Biol* 2005;25:6279-6288.
- 18 Kobayashi H: Suppression of urokinase expression and tumor metastasis by bikunin overexpression. *Hum Cell* 2001;14:233-236.
- 19 Kobayashi H, Gotoh J, Kanayama N, Hirashima Y, Terao T, Sugino D: Inhibition of tumor cell invasion through matrigel by a peptide derived from the domain II region in urinary trypsin inhibition. *Cancer Res* 1995;55:1847-1852.
- 20 Kobayashi H, Shinohara H, Gotoh J, Fujie M, Fujishiro S, Terao T: Anti-metastatic therapy by urinary trypsin inhibitor in combination with an anti-cancer agent. *Br J Cancer* 1995;72:1131-1137.
- 21 Kobayashi H, Shinohara H, Takeuchi K, Itoh M, Fujie M, Saitoh M, Terao T: Inhibition of the soluble and the tumor cell receptor-bound plasmin by urinary trypsin inhibitor and subsequent effects on tumor cell invasion and metastasis. *Cancer Res* 1994;54:844-849.
- 22 Kobayashi H, Suzuki M, Sun GW, Hirashima Y, Terao T: Suppression of urokinase-type plasminogen activator expression from human ovarian cancer cells by urinary trypsin inhibitor. *Biochim Biophys Acta* 2000;1481:310-316.
- 23 Yoshioka I, Tsuchiya Y, Aozuka Y, Onishi Y, Sakurai H, Koizumi K, Tsukada K, Saiki I: Urinary trypsin inhibitor suppresses surgical stress-facilitated lung metastasis of murine colon 26-L5 carcinoma cells. *Anticancer Res* 2005;25:815-820.
- 24 Yaguchi T, Muramoto M, Nakano T, Nishizaki T: Urinary trypsin inhibitor suppresses migration of malignant mesothelioma. *Cancer Lett* 2010;288:214-218.
- 25 Condeelis JS, Singer RH, Segall JE: The great escape: when cancer cells hijack the genes for chemotaxis and motility. *Annu Rev Cell Dev Biol* 2005;21:695-718.
- 26 Bertino P, Porta C, Barbone D, Germano S, Busacca S, Pinato S, Tassi G, Favoni R, Gaudino G, Mutti L: Preliminary data suggestive of a novel translational approach to mesothelioma treatment: imatinib mesylate with gemcitabine or pemetrexed. *Thorax* 2007;62:690-695.
- 27 Barbieri F, Würth R, Favoni RE, Pattarozzi A, Gatti M, Ratto A, Ferrari A, Bajetto A, Florio T: Receptor tyrosine kinase inhibitors and cytotoxic drugs affect pleural mesothelioma cell proliferation: insight into EGFR and ERK1/2 as antitumor targets. *Biochem Pharmacol* 2011;82:1467-1477.
- 28 Zucali PA, Ceresoli GL, De Vincenzo F, Simonelli M, Lorenzi E, Gianoncelli L, Santoro A: Advances in the biology of malignant pleural mesothelioma. *Cancer Treat Rev* 2011;37:543-558.

Heme Oxygenase-1 Promoter Polymorphism is Associated with Risk of Malignant Mesothelioma

Aki Murakami · Yoshihiro Fujimori · Yoshie Yoshikawa · Shusai Yamada · Kunihiro Tamura · Noriko Hirayama · Takayuki Terada · Kozo Kuribayashi · Chiharu Tabata · Kazuya Fukuoka · Tomoko Tamaoki · Takashi Nakano

Received: 17 March 2011 / Accepted: 4 January 2012 / Published online: 21 January 2012
© Springer Science+Business Media, LLC 2012

Abstract

Background Malignant mesothelioma is an aggressive tumor of serosal surfaces that is closely associated with asbestos exposure which induces oxidative stress. Heme oxygenase (HO)-1, a rate-limiting enzyme of heme degradation, plays a protective role against oxidative stress. The HO-1 gene promoter carries (GT)*n* repeats whose number is inversely related to transcriptional activity of the HO-1 gene.

Methods To investigate the relationship between the length polymorphism of (GT)*n* repeats and mesothelioma susceptibility, we analyzed the HO-1 promoter in 44 asbestos-exposed subjects without mesothelioma and 78 asbestos-exposed subjects with mesothelioma using PCR-based genotyping.

Results The number of repeats ranged from 16 to 38, with two peaks at 23 and 30 repeats. Polymorphisms of (GT)*n* repeats were grouped into two classes of alleles, short (S) (<24) and long (L) (≥24), and three genotypes: L/L, L/S, and S/S. The proportions of allele frequencies in class L as well as genotypic frequencies of L allele carriers

(L/L and L/S) were significantly higher in the asbestos-exposed subjects with mesothelioma than in those without mesothelioma.

Conclusion The findings of this study suggest that long (GT)*n* repeats in the HO-1 gene promoter are associated with a higher risk of malignant mesothelioma in the Japanese population.

Keywords Malignant mesothelioma · Heme oxygenase-1 · Polymorphism

Introduction

Malignant mesothelioma is an aggressive tumor that arises from mesothelial cells lining the pleural or peritoneal cavity. Mesothelioma is refractory to current therapies and associated with high mortality [1–3]. The development of mesothelioma is closely linked to the inhalation of asbestos fibers and characterized by a 30-year or greater latency period from the first exposure to asbestos.

The pathogenesis of asbestos-related mesothelioma is poorly understood. To explain the carcinogenic effect of inhaled asbestos fibers, it has been proposed that asbestos fibers induce the generation of free radicals and reactive oxygen species (ROS) and cause accumulation of DNA damage (oxidative stress theory) [4–6]. Antioxidant enzymes are induced after inhalation of asbestos, and the use of antioxidant scavengers has been shown to inhibit the toxic effect of asbestos [4, 5].

Heme oxygenase (HO) is an enzyme that catalyzes the breakdown of heme into carbon monoxide (CO), iron, and biliverdin which is then metabolized to bilirubin by biliverdin reductase [7–9]. Both biliverdin and bilirubin possess antioxidant properties [10]. CO has been shown to

A. Murakami · S. Yamada · K. Tamura · N. Hirayama · T. Terada · K. Kuribayashi · C. Tabata · K. Fukuoka · T. Nakano

Division of Respiratory Medicine, Department of Internal Medicine, Hyogo College of Medicine, 1-1 Mukogawa-cho, Nishinomiya, Hyogo 663-8501, Japan

Y. Fujimori (✉)
Hyogo College of Medicine, Cancer Center,
1-1 Mukogawa-cho, Nishinomiya, Hyogo 663-8501, Japan
e-mail: fuji-y@hyo-med.ac.jp

Y. Yoshikawa · T. Tamaoki
Department of Genetics, Hyogo College of Medicine,
1-1 Mukogawa-cho, Nishinomiya, Hyogo 663-8501, Japan

exhibit anti-inflammatory and antiapoptotic effects [11]. Mammalian heme oxygenase (HO) has three isoforms, HO-1, -2 and -3. HO-1 is highly induced by oxidative stress and confers protection against oxidant-induced injury [7–10].

The human HO-1 gene promoter contains a varying number of (GT)_n repeats ranging from 15 to 40 [12]. Longer (GT)_n repeats are associated with lower transcription of the HO-1 gene [13]. In polymorphic analysis, longer (GT)_n repeats in the HO-1 gene promoter are associated with increased risk of various diseases such as emphysema [14], asthma [15], diabetes mellitus [16], cardiovascular diseases [17], and cancers [18–22].

Although asbestos is closely associated with the risk of mesothelioma, there are some populations that do not develop mesothelioma after exposure to asbestos. In this study, we hypothesized that HO-1 gene variations may influence the susceptibility to mesothelioma. We report that length polymorphism in the HO-1 promoter is related to mesothelioma susceptibility. Our study could help to identify those with a higher risk of mesothelioma within a population exposed to asbestos fibers.

Materials and Methods

Patients' Characteristics

Forty-four asbestos-exposed subjects without mesothelioma and 78 asbestos-exposed subjects with mesothelioma were included in this study. All the mesothelioma patients were diagnosed at the Division of Respiratory Medicine, Department of Internal Medicine, Hyogo College of Medicine Hospital (Nishinomiya, Hyogo, Japan) between March 2000 and August 2007. The mesothelioma diagnosis was confirmed by histological and immunohistochemical examination of pleural biopsies obtained by thoracoscopy or thoracotomy. The presence of exposure to asbestos at the workplace, home, and other places was carefully recorded. Peripheral blood was collected from asbestos-exposed subjects by venipuncture. This study was approved by the institutional review board of Hyogo College of Medicine, and informed consent was obtained from each subject.

The subjects were categorized according to smoking history as current, ex-, or nonsmoker. Brinkman's index was calculated using the formula: the number of cigarettes/day × the number of years. Pulmonary emphysema was diagnosed based on a pulmonary function test [forced expiratory volume in 1.0 s (FEV_{1,0}) < 70%] and/or a computed tomography (CT) scan with the finding of low attenuation area (LAA). Diabetes mellitus type 2 was diagnosed according to the WHO criteria: fasting plasma glucose of 126 mg/dl or higher on more than two occasions, or symptoms of diabetes plus a casual plasma

glucose concentration of 200 mg/dl [23]. Hypertension was diagnosed based on systolic pressure >140 mmHg or a diastolic pressure equal to 90 mmHg or higher [24].

Analysis of Length Variability of (GT)_n Repeats in HO-1 Gene Promoter

Genomic DNAs were extracted from leukocytes by conventional procedures. The HO-1 promoter region containing a GT repeat was amplified by polymerase chain reaction (PCR) with a fluorescently labeled primer, p1-s (5'-AGAGCCTGCAGCTTCTCAGA-3'), and an unlabeled antisense primer, p1-as (5'-ACAAAGTCTGGCCATAG GAC-3') [14]. PCR was performed over 30 cycles of 20 s at 94°C, 10 s at 60°C, and 20 s at 72°C. The sizes of the PCR products were analyzed with a laser-based automated DNA sequencer (Applied Biosystems, Life Technologies, Carlsbad, CA, USA).

Statistical Analysis

Associations between subject groups and specific classes of alleles were analyzed for significance by the two-tailed χ^2 test. Associations between genotype groups were analyzed by two-tailed Fisher's exact probability test. Odds ratios and 95% confidence intervals (CIs) were calculated to assess the relative disease risk conferred by a particular allele and genotype. Statistical analysis of age and Brinkman's index was performed by unpaired *t*-test. Significance was accepted at $p < 0.05$.

Results

Clinical Characteristics of the Study Population

The clinical characteristics of 44 asbestos-exposed subjects without mesothelioma and 78 asbestos-exposed subjects with mesothelioma are given in Table 1. The smoking habits of those in the two groups did not differ significantly. Mean Brinkman's index for current and ex-smokers without mesothelioma and with mesothelioma was 791.9 and 804.2, respectively, not statistically different. Also, no significant differences were found between the two groups with respect to complications of pulmonary emphysema, cardiovascular disease, hypertension, and diabetes mellitus (Table 1).

Allele Frequencies of the HO-1 (GT)_n Dinucleotide Repeat Polymorphism

The allele frequencies of the (GT)_n repeats in the HO-1 promoter found in subjects without mesothelioma ($n = 44$,

Table 1 Characteristics of the study population

	Without mesothelioma (<i>n</i> = 44)	With mesothelioma (<i>n</i> = 78)	<i>p</i>
Age	66.7 (48–84)	64.8 (46–80)	0.913
Gender			
Male	33	58	0.937
Female	11	20	0.937
Smoking habit			
Current	19	35	0.856
Ex-smoker	11	15	0.454
Nonsmoker	14	28	0.648
Hypertension	10	23	0.419
Diabetes mellitus	4	13	0.374
Pulmonary emphysema	20	27	0.237
Cardiovascular disease	4	6	0.941

88 alleles) and subjects with mesothelioma (*n* = 78, 156 alleles) are shown in Fig. 1. The number of (GT)*n* repeats ranged from 16 to 38. In both groups, the distribution of the (GT)*n* repeats was bimodal, with one peak at 23 and the other at 30. We divided the alleles into two classes, short (S) alleles (<24) and long (L) alleles (≥24), according to the number of (GT)*n* repeats.

In the subjects without mesothelioma, the distribution of 88 alleles was 57 (64.8%) in class L and 31 (35.2%) in class S (Table 2). In subjects with mesothelioma, the distribution of 156 alleles was 123 (78.8%) in class L and 33 (21.2%) in class S. The proportion of allele frequencies in class L was significantly higher in the asbestos-exposed subjects with mesothelioma than in those without mesothelioma (*p* = 0.016, OR = 2.027, 95% CI = 1.132–3.628), indicating that L alleles are associated with a higher risk of mesothelioma, while S alleles are associated with a lower incidence of mesothelioma (OR = 0.493, 95% CI = 0.275–0.883) (Table 2).

Genotypic Frequencies

We then analyzed genotypic frequencies of the HO-1 promoter. The distribution of three genotypic frequencies (L/L, L/S, and S/S) is given in Table 3. These genotypes were divided into two subgroups: L allele carrier (L/L and L/S) and non-L allele carrier (S/S) (Table 3). The proportion of genotypic frequencies in L allele carriers (L/L + L/S) was significantly higher in subjects with mesothelioma than in those without mesothelioma (*p* = 0.025, OR = 6.00, 95% CI = 1.155–31.149) (Table 3). Furthermore, the odds ratio for mesothelioma was significantly higher in subjects with the L/L genotypes than in those with the S/S genotypes (for the L/L genotypes vs. the S/S genotypes, *p* = 0.015, OR = 7.421, 95% CI = 1.373–40.086) (Table 3). Thus,

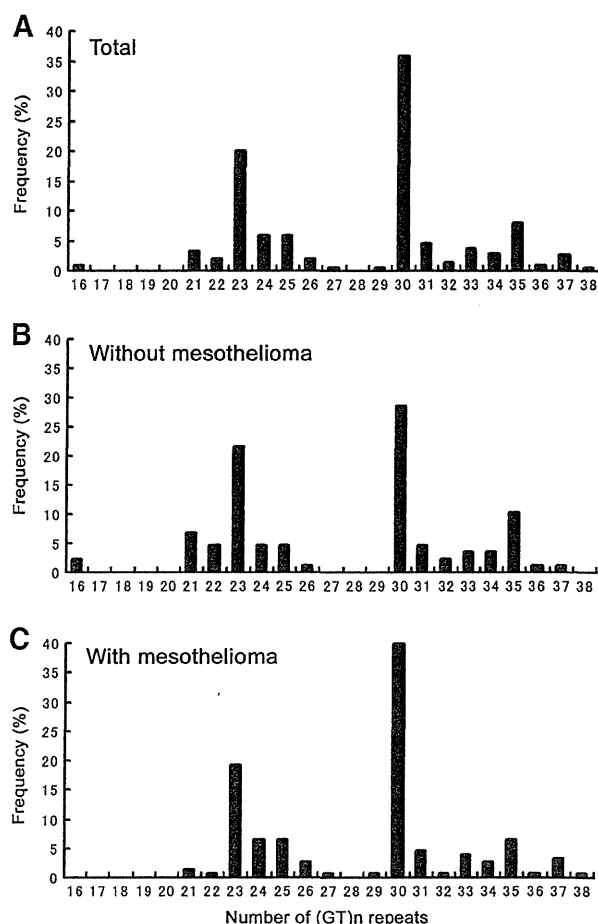


Fig. 1 Allele frequency distribution of the (GT)*n* repeats in the study subjects. **a** Total subjects (*n* = 122, 244 alleles). **b** Asbestos-exposed subjects without mesothelioma (*n* = 44, 88 alleles). **c** Asbestos-exposed subjects with mesothelioma (*n* = 78, 156 alleles)

Table 2 Allele frequencies at the polymorphic locus

Allele	Without mesothelioma (88 alleles)	With mesothelioma (156 alleles)	<i>p</i>	OR (95% CI)
L	57 (64.8%)	123 (78.8%)	0.016	2.027 (1.132–3.628)
S	31 (35.2%)	33 (21.2%)		0.493 (0.275–0.883)

OR odds ratio, 95% CI 95% confidence interval, S short alleles (<24 GT repeats), L long alleles (≥24 GT repeats)

genotypic frequencies of L allele carriers were associated with a higher risk of mesothelioma.

Discussion

Malignant mesothelioma is closely associated with asbestos exposure which causes oxidative stress [1–6]. Analysis of polymorphisms of glutathione S-transferase (GST) M1,

Table 3 Genotype subgroups at the polymorphic locus

Genotype subgroup	Without mesothelioma	With mesothelioma	<i>p</i>	OR (95% CI)
L/L	19 (43.2%)	47 (60.3%)	0.015*	7.421 (1.373–40.086)
L/S	19 (43.2%)	29 (37.2%)		
S/S (non-L allele carriers)	6 (13.6%)	2 (2.5%)		
L/L + L/S (L allele carriers)	38 (86.4%)	76 (97.5%)	0.025**	6.00 (1.155–31.149)

OR odds ratio, CI confidence interval, S short alleles (<24 GT repeats), L long alleles (≥24 GT repeats)

p values for * L/L genotypes versus S/S genotypes and ** L allele carriers (L/L + L/S) versus non-L allele carriers (S/S) by Fisher's exact probability test

an antioxidant enzyme, in relation to the risk of mesothelioma shows that a GST M1 null allele that exhibits no enzyme activity is associated with a higher risk of mesothelioma [25]. This finding supports the notion that antioxidant enzymes have a protective role against mesothelioma. In the present study, we evaluated the impact of HO-1 gene promoter polymorphisms on the risk of malignant mesothelioma.

HO-1, an inducible form of HO, provides cellular protection against heme- and non-heme-mediated oxidant injury [7]. The transcriptional upregulation of the HO-1 gene responds to many agents, including ROS. Asbestos also causes upregulation of heme oxygenase (HO) in human mesothelial cells [26], and intratracheal instillation of crocidolite asbestos induces HO-1 expression in rat lung tissues [27].

The human HO-1 gene has a varying number of GT repeats in the promoter [12–14]. Long (GT)_n repeats likely form the left-handed Z-DNA helix, reducing transcriptional activity of the HO-1 gene promoter [13]. It has been reported that promoter activity of the HO-1 gene containing short (GT)₂₂ repeats is four and eightfold higher than those containing longer (GT)₂₆ and (GT)₃₀ repeats, respectively [16]. After oxidative stimulation with H₂O₂, human lymphoblastoid cells possessing short (GT)_n repeats showed much higher activity of the HO-1 enzyme than cells carrying long repeats [28]. In addition, it has shown that longer (GT)_n repeats are a genetic risk factor for chronic pulmonary emphysema [14], coronary artery disease [16], and cancers such as lung adenocarcinoma [21] and oral squamous cell carcinoma [22].

In our study, 16–38 GT repeats of the HO-1 promoter showed a bimodal distribution, with two peaks at 23 and 30 (Fig. 1), which was consistent with previous reports in Japanese and Caucasian populations [16–22]. The incidence of hypertension, diabetes mellitus, emphysema, and cardiovascular disease, for which the risk of all has been shown to be associated with HO-1 promoter polymorphism, did not differ significantly statistically between subjects with mesothelioma and without mesothelioma (Table 1). The proportions of both allelic and genotypic frequencies of long (GT)_n repeats are higher in the

asbestos-exposed subjects with mesothelioma than in those without mesothelioma (Tables 2, 3). Long (GT)_n repeats are associated with lower HO-1 activity [13, 16, 28], which may result in reduced antioxidant activity and may contribute to a higher incidence of mesothelioma. Although our results were analyzed by using standard statistical methods, more definite proof would be provided by further analysis using Bayesian statistical methods. Currently, we do not have sufficient data on the population distribution of the (GT)_n repeats in our ethnic population; such analysis will be addressed in the future investigation.

In conclusion, the present study suggests that the long size of the (GT)_n repeat in the HO-1 gene promoter is associated with a higher risk of malignant mesothelioma in the Japanese population. This is the first report to document that the polymorphism in the HO-1 promoter gene is associated with mesothelioma susceptibility. However, oncogenesis is multifactorial and cannot be defined by a single-gene polymorphism. Further studies using a larger number of samples from different ethnicities are needed.

Acknowledgments We are grateful to Dr. Takashi Daimon (Department of Mathematics, Hyogo College of Medicine) for performing the statistical analysis. This study was supported by a Grant-in-Aid for Scientific Research from the Japan Society for the Promotion of Science, and in part by the Special Coordination Funds for Science and Technology from Japan Science and Technology Agency.

Conflict of interest The authors have no conflicts of interest to disclose.

References

1. Robinson BW, Musk AW, Lake RA (2005) Malignant mesothelioma. *Lancet* 366:397–408
2. Nakano T (2008) Current therapies for malignant pleural mesothelioma. *Environ Health Prev Med* 13:75–83
3. Baas P, Schouwink H, Zoetmulder FA (1998) Malignant pleural mesothelioma. *Ann Oncol* 9:139–149
4. Shukla A, Gulumian M, Hei TK, Kamp D, Rahman Q, Mossman BT (2003) Multiple roles of oxidants in the pathogenesis of asbestos-induced diseases. *Free Radic Biol Med* 34:1117–1129

5. Dong H, Buard A, Renier A, Lévy F, Saint-Etienne L, Jaurand MC (1994) Role of oxygen derivatives in the cytotoxicity and DNA damage produced by asbestos on rat pleural mesothelial cells in vitro. *Carcinogenesis* 15:1251–1255
6. Toyokuni S (2009) Mechanisms of asbestos-induced carcinogenesis. *Nagoya J Med Sci* 71:1–10
7. Otterbein LE, Choi AMK (2000) Heme oxygenase: colors of defense against cellular stress. *Am J Physiol Lung Cell Mol Physiol* 279:L1029–L1037
8. Okinaga S, Takahashi K, Takeda K, Yoshizawa M, Fujita H, Sasaki H, Shibahara S (1996) Regulation of human heme oxygenase-1 gene expression under thermal stress. *Blood* 87:5074–5084
9. Yamada N, Yamaya M, Okinaga S, Lie R, Suzuki T, Nakayama K, Takeda A, Yamaguchi T, Itoyama Y, Sekizawa K, Sasaki H (1999) Protective effects of heme oxygenase-1 against oxidant-induced injury in the cultured human tracheal epithelium. *Am J Respir Cell Mol Biol* 21:428–435
10. Choi AM, Alam J (1996) Heme oxygenase-1: function, regulation and implication of a novel stress-inducible protein in oxidant-induced lung injury. *Am J Respir Cell Mol Biol* 15:9–19
11. Otterbein LE, Bach FH, Alam J, Soares M, Tao LuH, Wysk M, Davis RJ, Flavell RA, Choi AM (2000) Carbon monoxide has anti-inflammatory effects involving the mitogen-activated protein kinase pathway. *Nat Med* 6:422–428
12. Exner M, Minar E, Wagner O, Schillinger M (2004) The role of heme oxygenase-1 promoter polymorphisms in human disease. *Free Radic Biol Med* 37:1097–1104
13. Shibahara S (2003) The heme oxygenase dilemma in cellular homeostasis: new insights for the feedback regulation of heme catabolism. *Tohoku J Exp Med* 200:167–186
14. Yamada N, Yamaya M, Okinaga S, Nakayama K, Sekizawa K, Shibahara S, Sasaki H (2000) Microsatellite polymorphism in the heme oxygenase-1 gene promoter is associated with susceptibility to emphysema. *Am J Hum Genet* 66:187–195
15. Islam T, McConnell R, Gauderman WJ, Avol E, Peters JM, Gilliland FD (2008) Ozone, oxidant defense genes, and risk of asthma during adolescence. *Am J Respir Crit Care Med* 177:388–395
16. Song F, Li X, Zhang M, Yao P, Yang N, Sun X, Hu FB, Liu L (2009) Association between heme oxygenase-1 gene promoter polymorphisms and type 2 diabetes in a Chinese population. *Am J Epidemiol* 170:747–756
17. Chen YH, Lin SJ, Lin MW, Tsai HL, Kuo SS, Chen JW, Charng MJ, Wu TC, Chen LC, Ding YA, Pan WH, Jou YS, Chau LY (2002) Microsatellite polymorphism in promoter of heme oxygenase-1 gene is associated with susceptibility to coronary artery disease in type 2 diabetic patients. *Hum Genet* 111:1–8
18. Hu JL, Li ZY, Liu W, Zhang RG, Li GL, Wang T, Ren JH, Wu G (2010) Polymorphism in heme oxygenase-1 (HO-1) promoter and alcohol are related to the risk of esophageal squamous cell carcinoma on Chinese males. *Neoplasma* 57:86–92
19. Huang SK, Chiu AW, Pu YS, Huang YK, Chung CJ, Tsai HJ, Yang MH, Chen CJ, Hsueh YM (2008) Arsenic methylation capability, heme oxygenase-1 and NADPH quinone oxidoreductase-1 genetic polymorphisms and the stage and grade of urothelial carcinomas. *Urol Int* 80:405–412
20. Sawa T, Mounawar M, Tatemichi M, Gilibert I, Katoh T, Ohshima H (2008) Increased risk of gastric cancer in Japanese subjects is associated with microsatellite polymorphisms in the heme oxygenase-1 and the inducible nitric oxide synthase gene promoters. *Cancer Lett* 269:78–84
21. Kikuchi A, Yamaya M, Suzuki S, Yasuda H, Kubo H, Nakayama K, Handa M, Sasaki T, Shibahara S, Sekizawa K, Sasaki H (2005) Association of susceptibility to the development of lung adenocarcinoma with the heme oxygenase-1 gene promoter polymorphism. *Hum Genet* 116:354–360
22. Chang KW, Lee TC, Yeh WI, Chung MY, Liu CJ, Chi LY, Lin SC (2004) Polymorphism in heme oxygenase-1 (HO-1) promoter is related to the risk of oral squamous cell carcinoma occurring on male areca chewers. *Br J Cancer* 91:1551–1555
23. Kuzuya T, Nakagawa S, Satoh J, Kanazawa Y, Iwamoto Y, Kobayashi M, Nanjo K, Sasaki A, Seino Y, Ito C, Shima K, Nonaka K, Kadowaki T, Committee of the Japan Diabetes Society on the diagnostic criteria of diabetes mellitus (2002) Report of the Committee on the classification and diagnostic criteria of diabetes mellitus. *Diabetes Res Clin Pract* 55:65–85
24. Alderman MH (1993) A review of the Joint National Committee on detection, evaluation, and treatment of high blood pressure. The fifth report, 1993. *Am J Hypertens* 6:896–898
25. Landi S, Gemignani F, Neri M, Barale R, Bonassi S, Bottari F, Canessa PA, Canzian F, Ceppi M, Filiberti R, Ivaldi GP, Mencoboni M, Scaruffi P, Tonini GP, Mutti L, Puntoni R (2007) Polymorphisms of glutathione-S-transferase M1 and manganese superoxide dismutase are associated with the risk of malignant pleural mesothelioma. *Int J Cancer* 120:2739–2743
26. Janssen YM, Marsh JP, Absher MP, Gabrielson E, Borm PJ, Driscoll K, Mossman BT (1994) Oxidant stress responses in human pleural mesothelial cells exposed to asbestos. *Am J Respir Crit Care Med* 149:795–802
27. Nagatomo H, Morimoto Y, Oyabu T, Hirohashi M, Ogami A, Yamato H, Kuroda K, Higashi T, Tanaka I (2005) Expression of heme oxygenase-1 in the lungs of rats exposed to crocidolite asbestos. *Inhal Toxicol* 17:293–296
28. Hirai H, Kubo H, Yamaya M, Nakayama K, Numasaki M, Kobayashi S, Suzuki S, Shibahara S, Sasaki H (2003) Microsatellite polymorphism in heme oxygenase-1 gene promoter is associated with susceptibility to oxidant-induced apoptosis in lymphoblastoid cell lines. *Blood* 102:1619–1621

Frequent inactivation of the *BAP1* gene in epithelioid-type malignant mesothelioma

Yoshie Yoshikawa,^{1,6} Ayuko Sato,² Tohru Tsujimura,² Mitsuru Emi,^{1,3} Tomonori Morinaga,¹ Kazuya Fukuoka,⁴ Shusai Yamada,⁴ Aki Murakami,⁴ Nobuyuki Kondo,⁵ Seiji Matsumoto,⁵ Yoshitomo Okumura,^{5,7} Fumihiro Tanaka,⁵ Seiki Hasegawa,⁵ Takashi Nakano⁴ and Tomoko Hashimoto-Tamaoki¹

¹Department of Genetics; ²Division of Molecular Pathology, Department of Pathology, Hyogo College of Medicine, Hyogo, Japan; ³Division of Thoracic Oncology & Cancer Biology, University of Hawaii Cancer Center, Honolulu, Hawaii, USA; and ⁴Division of Respiratory Medicine, Department of Internal Medicine, and ⁵Department of Thoracic Surgery, Hyogo College of Medicine, Hyogo, Japan

(Received October 25, 2011/Revised January 16, 2012/Accepted January 17, 2012/Accepted manuscript online February 9, 2012/Article first published online February 21, 2012)

In the present study, we analyzed genomic alterations of BRCA1-associated protein 1 (*BAP1*) in 23 malignant mesotheliomas (MMs), 16 epithelioid and seven non-epithelioid, consisting of 18 clinical specimens and five established cell lines. In examining these samples for homozygous deletions and sequence-level mutations, we found biallelic *BAP1* gene alterations in 14 of 23 MMs (61%). Seven of these 14 MMs had homozygous deletions of the partial or entire *BAP1* gene, another five had sequence-level mutations, including small deletions, a nonsense mutation, and missense mutations with additional monoallelic deletions, and the remaining two had homozygous mutations without allelic loss. All but one of the 14 *BAP1* gene mutations were found in the epithelioid-type MMs; *BAP1* mutations were found in 13 of 16 epithelioid-type MMs, but in only one of seven non-epithelioid-type MMs (13/16 vs 1/7; $P = 0.005$). There was no *BAP1* mRNA expression in MMs with biallelic deletion and repressed expression was confirmed in MM specimens with deletion/mutation as compared with Met5a, SV40-transformed normal mesothelial cells. Western blot showed that seven of eight epithelioid MMs analyzed were *BAP1* negative. Immunostaining with anti-*BAP1* antibody in normal lung tissues revealed clear nuclear staining of normal mesothelial cells. No nuclear staining was observed among *BAP1* mutation-positive MM tumors, whereas nuclear staining was observed among *BAP1* mutation-negative MM tumors. These results suggest that the lack of the tumor suppressor *BAP1* may be more specifically involved in the pathogenesis of epithelioid MM rather than non-epithelioid MM, and would be useful for diagnosis of epithelioid-type MM. (*Cancer Sci* 2012; 103: 868–874)

Malignant mesothelioma (MM) is an asbestos-related malignancy that arises primarily from surface serosal cells of pleural, peritoneal, and pericardial cavities. Although the use of asbestos has decreased in Western countries and Japan, the incidence of MM is expected to increase over the next few decades because of the long latency period (20–40 years) of this malignancy.⁽¹⁾ Although the prognosis of MM is generally poor, epithelioid-type MM has been reported to be associated with better prognosis than non-epithelioid types of MM.⁽²⁾ Multiple modality approaches involving surgery with radiation, chemotherapy, or immunotherapy have generated favorable outcomes, particularly for patients with epithelioid-type MM.⁽³⁾

One of the most common genetic alterations in MM is homozygous deletion of the 9p21 locus containing the *CDKN2A* and *CDKN2B* genes.^(4,5) The *NF2* gene is also often mutated in MM.^(6,7) Conversely, mutations of the *p53*, *Ras*, and *RB* genes, common in many other types of tumors, are very rare in MM.^(8,9) Previously, using Comparative Genomic

Hybridization (CGH) array, we found that more than half of MM samples exhibit homozygous and heterozygous deletions of 3p21.1.⁽¹⁰⁾ Three of our MM cases, namely MM21-P, MM34-P, and MM14-T, had homozygous deletions at 3p21.1. The overlapping homozygous deletion in these cases was approximately 160 kb in length, spanning nine genes and including BRCA1-associated protein 1 (*BAP1*).⁽¹⁰⁾ Initially, *BAP1* was identified as a protein that binds to the RING finger domain of BRCA1 and exhibits tumor-suppressor activity in cancer cells.^(11,12) It is one of the cysteine proteases called deubiquitinating enzymes that catalyze the removal of ubiquitin chains from ubiquitinated proteins. It has been reported recently that *BAP1* is frequently mutated in metastasizing uveal melanoma, but not in low-metastatic uveal melanoma.⁽¹³⁾ Herein, we report on genomic alterations of *BAP1*.

Materials and Methods

MM cells and tissue specimens. Pleural effusions, ascites, and tumor tissues were obtained from 18 patients diagnosed with MM by pathological examination at the hospital of Hyogo College of Medicine. Matched peripheral blood was obtained from 11 patients (see Table S1), but matched normal tissues from the other seven patients were unavailable. All patients provided written informed consent. The human normal pleura transformant cell line Met5a (used as a reference) and four MM cell lines (i.e. H2052, H2452, H28, and MSTO-211H) were obtained from the American Type Culture Collection (ATCC; Rockville, MD, USA). The HMMME cell line was obtained from the Riken Bioresource Center (Tsukuba, Japan). The characteristics of these cells are given in Table S1.

Cells in pleural effusions and ascites were collected by centrifugation and cultured in α -Minimal Essential Medium (α -MEM; Invitrogen, Carlsbad, CA, USA) supplemented with 10% FBS (Equitech-Bio, Ingram, TX, USA). Surgically resected tumors were cut into small pieces and used for plating on culture dishes for growth. Primary outgrowth cells were cultured in α -MEM–10% FBS and adherent cells were expanded by several passages. These cells were termed MM primary cell cultures (MM-Ps) and 16 MM-Ps were used in the present study. For cases MM14 and MM29, primary cell cultures were not established; in these cases, tissue specimens (termed MM-Ts) were used for analysis. Tumor tissues resected from all but one MM patient (17 of 18 cases; a tissue specimen was unavailable for MM34), and lung tissues of one patient with pulmonary emphysema were fixed with 10%

⁶To whom correspondence should be addressed.

E-mail: yoshiey@hyo-med.ac.jp

⁷Present address: Itami City Hospital, Hyogo, Japan.

formalin, and embedded in paraffin for subsequent immunohistochemistry.

The present study was approved by the Ethics Committee of Hyogo College of Medicine and was performed in accordance with the Declaration of Helsinki (1995) as revised in Tokyo in 2004.

Reagents. Anti-BAP1 antibody (C-4; sc-28383) was obtained from Santa Cruz Biotechnology (Santa Cruz, CA, USA), ACTB (Sc-74; A5316) was from Sigma-Aldrich (St. Louis, MO, USA), and horseradish peroxidase-conjugated secondary antibody for enhanced chemiluminescence (ECL) was from GE Healthcare (Waukesha, WI, USA).

Extraction of DNA and RNA and real-time RT-PCR. In the present study, DNA and RNA were isolated from cultured cells, tissues, and peripheral blood using the AllPrep DNA/RNA mini kit (Qiagen, Hilden, Germany) according to the manufacturer's instructions. For MM cells, real-time RT-PCR was performed to analyze gene expression using 2 ng cDNA (reverse transcribed from total RNA) and the following primer: for *BAP1*, 5'-AGGAGCTGCTGGCACTGCTGA-3' (sense) and 5'-TTGTGGAGCCGGCCGATGCT-3' (antisense); and for *GAPDH*, 5'-GCACCGTCAAGGCTGAGAAC-3' (sense) and 5'-TGGTGAAGCGC-CAGTGGGA-3' (antisense). Gene expression was normalized against that of *GAPDH* and the expression of *BAP1* in MM samples was compared with that in Met5a cells.

Screening for genomic alterations. Genomic DNA, extracted as described above, was amplified by PCR using primers for the coding region of *BAP1* (Table 1). Amplified products were analyzed for direct sequencing using Big Dye Terminator v3.1 on an Applied Biosystems 3130 Genetic Analyzer (Applied Biosystems, Foster, CA, USA). The following primer set was used to detect exon 9 in *BAP1*: 5'-CTGTGACTGCAGGGA-GCCCTACCA-3' (sense) and 5'-AAGGGCACCTACCTGCTGCAGAG-3' (antisense).

Western blotting. Cell lysates were prepared using lysis buffer (Cell Signaling Technology, Danvers, MA, USA) and 5 µg isolated protein was electrophoresed on a 10–20% TGX gel (Bio-Rad, Hercules, CA, USA). Proteins were transferred onto polyvinylidene difluoride membranes and blocked with 5% non-fat powdered milk in 1× Tris-buffered saline with 0.1% Tween-20 (TBS-T) for 30 min. Membranes were washed with TBS-T, incubated with primary antibody for 2 h, followed by incubation with the secondary antibody for 1 h, and developed

using an ECL Plus Western Blotting Detection System (GE Healthcare).

Immunohistochemistry. Formalin-fixed, paraffin-embedded MM tissues were cut into 4-µm sections. Sections were heated in Target Retrieval Solution (S1700; DakoCytomation, Glostrup, Denmark) at 98°C for 25 min to facilitate antigen retrieval. After blocking with goat serum, sections were incubated with mouse anti-BAP1 antibody (1:50 dilution) for 30 min and then with EnVision FLEX + Mouse (LINKER) including rabbit polyclonal antibody to mouse immunoglobulin (K8022; DakoCytomation) for 15 min to increase the sensitivity of detection. This was followed by treatment with goat polyclonal antibodies to rabbit and mouse immunoglobulin for 30 min using Chem-Mate EnVision Kit (K5007; DakoCytomation) and visualization with 3,3'-diaminobenzidine tetrahydrochloride. Cells were lightly stained with hematoxylin.

Statistical analysis. Fisher's exact test was used for statistical comparisons of biallelic mutation frequencies between the two groups (epithelioid MMs versus non-epithelioid MMs). $P \leq 0.05$ was considered significant.

Results

Genomic alterations of the *BAP1* gene are frequently seen in MM cells. To examine homozygous deletion and sequence-level mutations in the *BAP1* gene, PCR was used to amplify 10 fragments, derived from the entire coding region of this gene, in 23 MM samples: 18 from patients with MM (16 MM-Ps and two MM-Ts) attending the hospital of Hyogo College of Medicine, four MM cell lines obtained from the ATCC, and one cell line obtained from RIKEN. These samples consisted of 16 epithelioid-type MMs and seven non-epithelioid MMs. We found biallelic *BAP1* gene alterations in 14 of 23 MMs (61%; Table 2). For MM19-P, MM21-P, MM34-P, and MM14-T, no amplification was identified using the primer pairs described in Table 1 (Fig. 1a,b). Surprisingly sequence analysis detected many genomic alterations in both our MM cases and the commercial MM cell lines (Table 2; Fig. 1) as follows: (i) deletions of exons 1–5 causing loss of the N terminal region (MM39-P and MM48-P); (ii) deletion of exons 10–17 causing premature protein termination (MM57-P); (iii) deletion of three nucleotides in exon 9 (MM29-T); (iv) frameshift mutations causing premature protein termination

Table 1. Sequences of the primers used in the present study to amplify the 10 fragments for sequencing of the *BAP1* coding region

Fragment	Target	Primer design region	Primer sequence
1	Exon 1–3	Exon 1 Intron 3	Forward: 5'-CCGTGTGCTGTGTGTGGGACTGAG-3' Reverse: 5'-AGAGCAAGGCTGCTCTTTCTGTG-3'
2	Exon 4	Intron 3 Intron 4	Forward: 5'-CACCTGAGTGATGACGCAGTGCAA-3' Reverse: 5'-TACCCACTGGATATCTGAGGACAC-3'
3	Exon 5	Intron 4 Intron 5	Forward: 5'-TAGGAGGGTGTCTGAGTCCACTC-3' Reverse: 5'-CAGATCTGCCAGTTGGCTGTGAG-3'
4	Exon 6–7	Intron 5 Intron 7	Forward: 5'-CCACCCATAGTCTACTCG-3' Reverse: 5'-AACAGGCCCTCCAGCTCATGGTG-3'
5	Exon 8	Exon 7 Intron 8	Forward: 5'-GGCTGAAGGTCTACCCCATGAC-3' Reverse: 5'-CCAGATTCACCATATGGCCTTGCA-3'
6	Exon 9–10	Intron 8 Intron 10	Forward: 5'-GTGCCTGGCATGTATGGC-3' Reverse: 5'-CCTCCATGTGACACATTAG-3'
7	Exon 11	Intron 10 Intron 11	Forward: 5'-TTCTCTGGGAAGTGCTGGTT-3' Reverse: 5'-GGAACCATGGAATAATTG-3'
8	Exon 12	Intron 11 Intron 12	Forward: 5'-CAAGGACAGGCCATGGAAC-3' Reverse: 5'-AGGTGCTCAACATTATCTGC-3'
9	Exon 13–14	Intron 12 Intron 14	Forward: 5'-CATTCTGGGTACTGCTGGGT-3' Reverse: 5'-CCACCAATCTTACACCAAAA-3'
10	Exon 15–17	Intron 14 Exon 17	Forward: 5'-TCCTTGCTCTAGCTGCCTAT-3' Reverse: 5'-TACTGGGAAAAGGGGAAGTG-3'

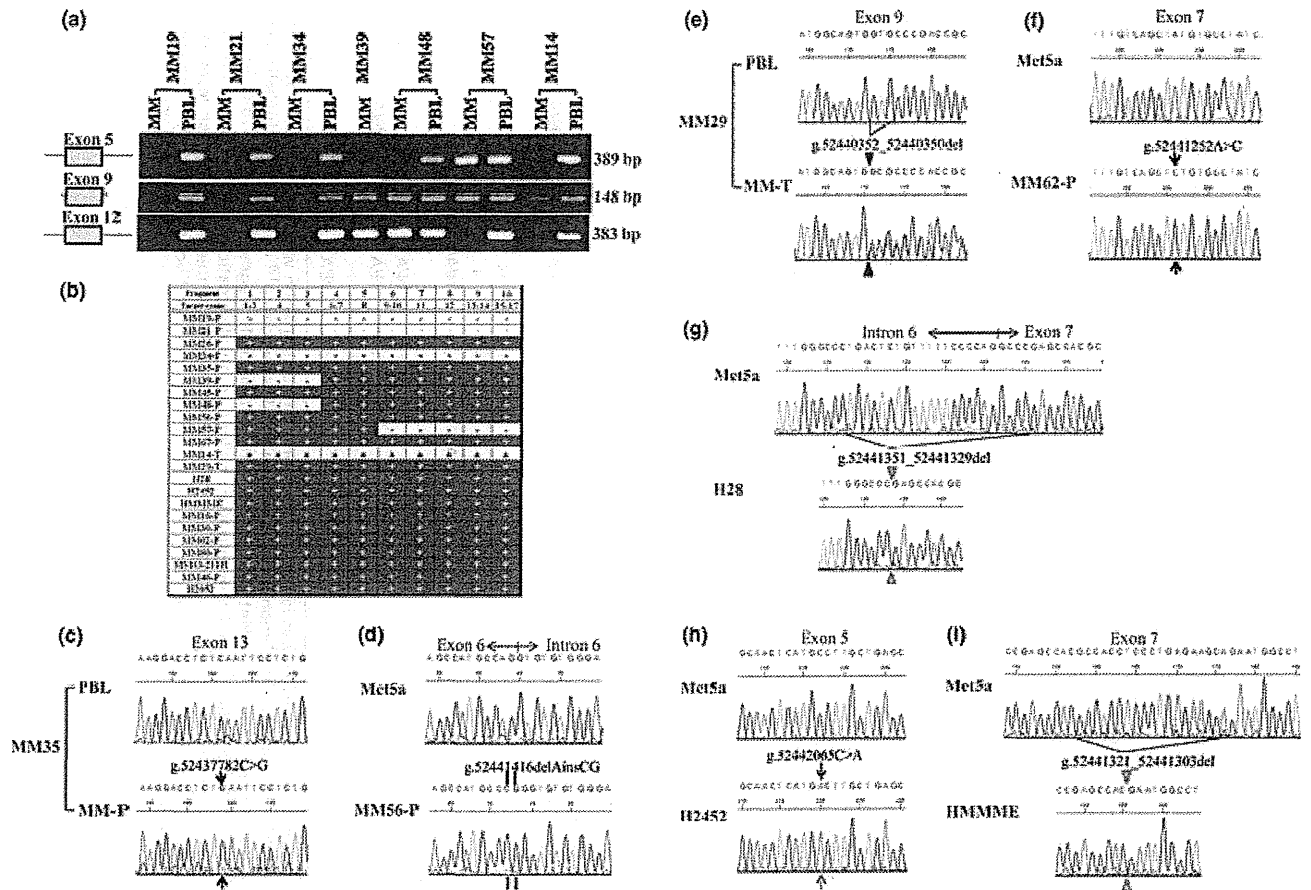


Fig. 1. Genomic alterations of the *BAP1* gene. (a) Agarose gel electrophoresis of PCR fragments amplified with the primers detecting exon 5 (fragment 3 in Table 1), exon 9, and exon 12 of *BAP1* (fragment 8) from patients with malignant mesothelioma (MM19, MM21, MM34, MM39, MM48, MM57, and MM14). MM, tumor sample of malignant mesothelioma; PBL, matched normal peripheral blood leukocyte. (b) Summary of amplification of each PCR fragment using primers for the coding region of *BAP1* in each sample we analyzed. +, amplified; ±, a slight amplification; -, not amplified; MM-Ps, MM primary cell cultures; MM-Ts, tissue specimens. (c) Electropherogram showing *BAP1* nonsense mutation (g.52437782C>G) within exon 13 in MM35-P. (d) Electropherogram showing *BAP1* insertion/deletion mutation (g.5244116delAinsCG) within exon 6 in MM56-P. (e) Electropherogram showing a 3-bp deletion (g.52440352_52440350del) within exon 9 in MM29-T. (f) Electropherogram showing *BAP1* missense mutation (g.52441252A>C) within exon 7 in MM62-P. (g) Electropherogram showing 23-bp deletion (g.52441351_52441329del) at the intron 6-exon 7 boundary in the H28 cell line. (h) Electropherogram showing *BAP1* missense mutation (g.52442065C>A) within exon 5 in the MM cell line H2452. (i) Electropherogram showing a 19-bp deletion (g.52441321_52441303del) within exon 7 in the MM cell line HMMME.

due to insertion/deletion (MM56-P) or deletion of 19 nucleotides (HMMME); (v) deletion of 23 nucleotides causing loss of a splice acceptor site (H28); (vi) nonsense mutation (MM35-P); and (vii) missense mutation (MM62-P and H2452). Sequence data for samples carrying these mutations were not heterogeneous (Fig. 1c,d,f-i), with the exception of MM29-T, which likely appeared heterogeneous owing to contamination by normal tissue (Fig. 1e). Biallelic alteration of the *BAP1* gene was then identified by PCR and sequencing analysis for the 14 mutated MMs. Our CGH array data⁽¹⁰⁾ supported these results (Table 2). Seven MM cases (i.e. MM19-P, MM21-P, MM34-P, MM39-P, MM48-P, MM57-P, and MM14-T) had biallelic deletions in *BAP1*. For MM35-P, MM56-P, MM29-T, H2452, and HMMME, biallelic alterations in this gene were caused by sequence-level mutations and loss of the remaining allele, and both H28 and MM62-P had biallelic mutations. Allelic changes of the *BAP1* gene were deletion/deletion (six MM-Ps, two MM-Ts, and two MM lines), deletion/insertion and deletion (one MM-P), deletion/base substitution (one each MM-P and MM line), and base substitution/base substitution (one MM-P; Fig. 2). Thus, the biallelic deletions were most

frequently found for *BAP1* inactivation. With the exception of the nonsense mutation at amino acid position 460 (p.S460X) in MM35-P, the other six sequence-level mutations occurred in the ubiquitin carboxyl terminal hydrolase domain (Fig. 2). Mutations in MM56-P (p.R146RfsX9), H28, and HMMME (p.R150RfsX31) induced premature termination, and ones in MM29-T (p.V234del) and MM62-P (p.Y173S) occurred at positions close to the active site of the enzyme. A missense mutation at amino acid position 95 (p.A95D), which is known to impair deubiquitinase activity,⁽¹⁴⁾ was found in H2452.

All but one of 14 *BAP1* gene mutations were found among epithelioid-type MMs, and MM62-P was the only non-epithelioid MM showing genomic alterations in *BAP1*. Mutations in *BAP1* were found in as many as 13 of 16 epithelioid MMs (81%). Statistical analysis indicated that the frequency of biallelic mutations in epithelioid-type MM was significantly higher than that in non-epithelioid-type MM ($P = 0.005$).

These genomic alterations in the *BAP1* gene were judged as somatic in nine cases because no such alterations were found

Table 2. Summary of *BAP1* gene alterations in malignant mesothelioma

Histological type	Specimen	Source	Allelic status of 3p21.1 (position: 52.4–52.6 Mb)	Genomic alterations in <i>BAP1</i>			<i>BAP1</i> expression		
				Mutation in the coding region	Somatic alteration	mRNA	Protein	Nuclear immunostaining in tumor tissue	
Epithelioid	MM19-P	HCM	-/+	Deletion of <i>BAP1</i> coding region	+	-	-	-	
	MM21-P	HCM	-/-	Deletion of entire <i>BAP1</i> gene	+	-	-	-	
	MM26-P	HCM	+/+	ND	-	++	++	+	
	MM34-P†	HCM	-/-	Deletion of entire <i>BAP1</i> gene	+	-	N/A	N/A	
	MM35-P	HCM	-/+	Nonsense mutation at aa 460 (g.52437782C>G, p.S460X)	+	±	-	-	
	MM39-P	HCM	-/+	Deletion of exons 1–5	N/A	-	-	-	
	MM45-P	HCM	-/+	ND	+	+	N/A	-	
	MM48-P	HCM	-/+	Deletion of exons 1–5	+	-	-	-	
	MM56-P	HCM	-/+	Frameshift mutation at aa146 (g.52441416delAinsCG, p.R146RfsX9)	N/A	±	-	‡	
	MM57-P	HCM	-/+	Deletion of exons 10–17	+	-	N/A	-	
	MM67-P	HCM	+/+	ND	-	+	N/A	++	
	MM14-T	HCM	-/-	Deletion of entire <i>BAP1</i> gene	+	N/A	N/A	-	
	MM29-T	HCM	-/+	3-bp deletion at aa234 (g.52440352_52440350del, p.V234del)	+	N/A	N/A	-	
	H28	ATCC	+/+	23-bp deletion at intron 6/exon7 junction§ (g.52441351_52441329del)	N/A	++	N/A	N/A	
	H2452	ATCC	-/+	Missense mutation at aa95 (g.52442065C>A, p.A95D)	N/A	++	-	N/A	
HMMMME	RIKEN	-/+	19-bp deletion (g.52441321_52441303del, p.R150RfsX31)	N/A	+	N/A	N/A		
Non-epithelioid (biphasic)	MM16-P	HCM	+/+	ND	-	++	++	+	
	MM30-P	HCM	+/+	ND	-	++	+	+	
	MM62-P	HCM	+/+	Missense mutation at aa 173§ (g.52441252A>C, p.Y173S)	N/A	++	N/A	-	
	MM80-P	HCM	+/+	ND	-	++	N/A	+	
	MSTO-211H	ATCC	+/+	ND	-	+	N/A	N/A	
Non-epithelioid (sarcomatoid)	MM46-P	HCM	+/+	ND	-	++	++	+	
	H2052	ATCC	+/+	ND	-	++	N/A	N/A	

†This specimen was unavailable for protein analysis. ‡Nuclear staining was seen in some tumor cells, but not all. §This was identified as a homozygous mutation without allelic loss by direct sequencing. The allelic status of 3p21.1 (position: 52.4–52.6 Mb), identified from our previously published Comparative Genomic Hybridization (CGH) array data,⁽¹⁰⁾ is shown, and biallelic and monoallelic deletion of this region is indicated by -/- and -/+, respectively. Mutations in the *BAP1* coding region were identified by direct sequencing of 10 fragments, derived from the entire coding region of this gene and amplified using the primers described in Table 1. For somatic alterations, the "+" indicates mutations judged to be of somatic origin of the nine malignant mesotheliomas (MMs) for which comparisons with paired non-tumor DNA were possible and "-" indicates no mutations in the coding region. For *BAP1* expression, expression level data summarized from Figure 3 are shown as - (no expression), ±, +, or ++ (similar as that in Met5a cells). Immunohistochemistry was performed using an anti-BAP1 antibody for primary tissue specimens and nuclear immunostaining is indicated as -, +, and ++ (similar as that in non-tumor mesothelial cells shown in Fig. 4a). aa, amino acid; HCM, Hyogo College of Medicine; ND, not detected; N/A, not analyzed.

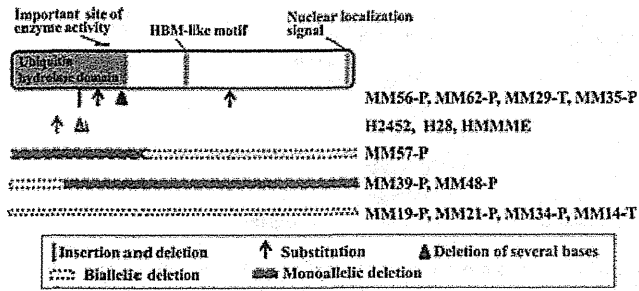


Fig. 2. Summary of mutation sites in *BAP1* for the samples from patients and cell lines showing biallelic alterations and the site of functional domain or motif. HBM, HCF-binding motif.

in DNA from the available matched peripheral blood samples. However, the other three cases were unidentified because of the unavailability of matched normal tissue.

Repressed expression of the *BAP1* gene in MM cells. Real-time RT-PCR was conducted on 16 MM-Ps and five commercial MM cell lines. The results indicated no expression of *BAP1* mRNA in six of 16 MM-Ps due to biallelic deletion of this gene (MM19-P, MM21-P, MM34-P, MM39-P, MM48-P, and MM57-P; Fig. 3a). Suppression of *BAP1* mRNA expression in three MM-Ps and one cell line was observed due to deletions/mutations (in MM35-P, MM56-P, and HMMME) and monoallelic deletion (in MM45-P). Moreover, both MM67-P and MSTO-211H, which had no verifiable genomic changes in the coding region of *BAP1*, showed suppression of *BAP1* expression (Fig. 3a). Western blotting showed complete absence of BAP1 protein in MM-Ps with biallelic gene deletion (MM19-P, MM21-P, MM39-P, and MM48-P), and loss of one allele combined with mutation (MM35-P and H2452) or combined with insertion and deletion (MM56-P; Fig. 3b). Immunohistochemistry with anti-BAP1 antibody showed nuclear staining in non-tumor mesothelial cells on the lung surface (Fig. 4a) and in tumor cells of MM tissue specimens with the wild-type *BAP1* (MM26, MM67, MM16, MM30, MM80, and MM46; Fig. 4b). No nuclear staining was observed in tumor cells from which MMs with *BAP1* alterations were established (MM19, MM21, MM35, MM39, MM45, MM48, MM57, MM14, MM29, and MM62; Fig. 4c).

It should be noted that some tumor cells of MM56, but not all, showed nuclear staining.

Discussion

In the present study, we found frequent somatic alterations in the *BAP1* locus in Japanese patients with MM. Fourteen of our 23 MM samples had various types of biallelic genomic alterations in *BAP1*, including deletions encompassing the whole *BAP1* locus or involving several exons (Table 2). Biallelic alterations are generally caused by monoallelic mutations coupled with monoallelic loss, and, although our data indicated that both H28 and MM62-P had homozygous mutations without allelic loss, we were unable to prove this. However, the ratio of the copy numbers of exon 13 determined by quantitative real-time PCR and of the probes designed for the *BAP1* region in the CGH array suggest that these MM cells have no allelic deletions in this gene region (Table S2). No expression or decreased expression of *BAP1* mRNA was frequently observed in epithelioid-type MM cells. In addition, *BAP1* gene expression was repressed in MM45-P and MM67-P, with monoallelic deletion of *BAP1* found by real-time PCR (Table S2). Monoallelic deletion in MM45-P has been identified previously by paired CGH array analysis using matched peripheral blood samples,⁽¹⁰⁾ however, we were unable to conclusively demonstrate monoallelic loss in MM67-P because of the unavailability of matched normal tissue.

While we were preparing this manuscript for publication, four papers were published showing that somatic and germline mutations of *BAP1* predispose to MM and other types of tumors.^(15–18) Bott *et al.*⁽¹⁵⁾ reported that 12 of 53 MM tumors (23%) collected in the US had somatic inactivating mutations of *BAP1*. Six of 12 had monoallelic loss of 3p21.1 with mutations in the remaining allele. Testa *et al.*⁽¹⁷⁾ found germline *BAP1* mutations in two US families with a high incidence of MM. The affected members of one family had a base substitution at the intron 6–exon 7 boundary in germline DNA, whereas those of another family had a common nonsense mutation in exon 16 in germline DNA. In these affected members, somatic *BAP1* alterations developed in the remaining allele, leading to biallelic inactivation of this gene. Testa *et al.*⁽¹⁷⁾ also found germline *BAP1* mutations in two of 26 sporadic MMs, and these mutations showed 1- or 4-bp deletions in exon 13 or 14, respectively, resulting in frameshift leading to a stop codon. Other studies

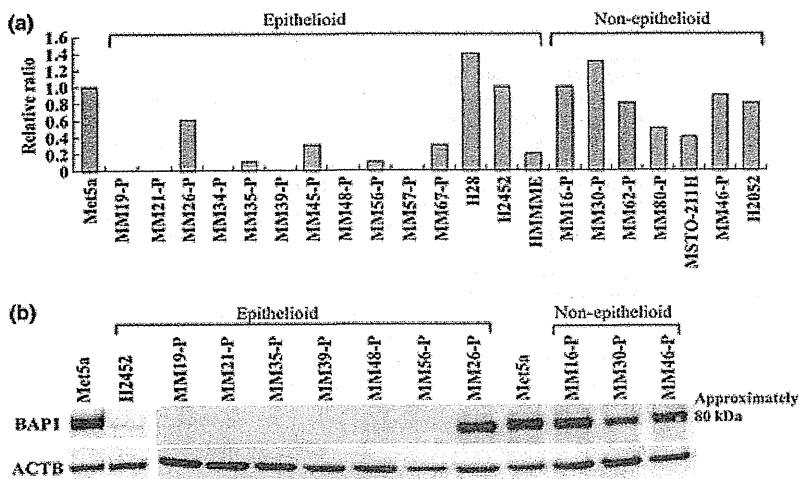


Fig. 3. Repressed expression of *BAP1* gene. (a) Gene expression of *BAP1* in malignant mesothelioma (MM) cells, analyzed by real-time RT-PCR and normalized against GAPDH, is presented as a ratio relative to expression in Met5a cells. (b) Western blotting. Expression of BAP1 protein was examined in Met5a cells, H2452 cells, and primary cell cultures obtained from seven patients with epithelioid MM and three patients with non-epithelioid MM. β -actin (ACTB) was used as a positive control.

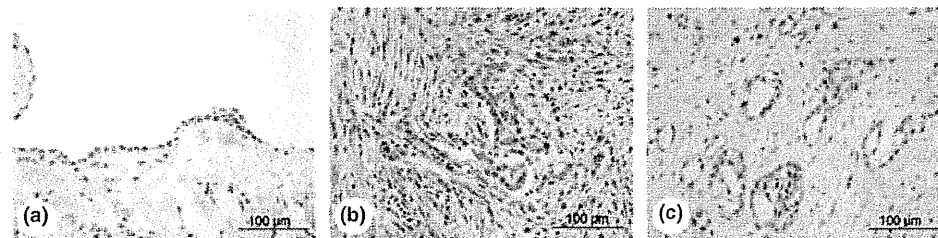


Fig. 4. Immunostaining with anti-BAP1 antibody. (a) A specimen of the lung surface of a patient with pulmonary emphysema. (b) A specimen of tumors from patient MM80, who had biphasic malignant mesothelioma (MM). (c) A specimen of tumors from patient MM35, who had epithelioid MM.

reported that families with a high incidence of melanocytic tumors⁽¹⁶⁾ and several tumors, including MM,⁽¹⁸⁾ carry various somatic alterations in addition to inactivating germline mutations of *BAP1*. In the biallelic deletions we found, the length of deletion differed between two alleles, with the exception of H28. These results suggest that *BAP1* is subject to loss-of-function mutations (especially two-step alterations) because of inherent instability, although no particular mutation hotspots are apparent. Our findings reveal that *BAP1* gene inactivation occurs at a very high frequency in patients with epithelioid MM, the most common form of MM, and that this may be useful for a diagnosis of MM. In contrast, Bott *et al.*⁽¹⁵⁾ could not find any significant correlation between somatic mutations of *BAP1* and histological type. The rare case in the present study was MM62-P, who had biphasic MM consisting of epithelioid and sarcomatoid types. It is interesting that, in previous reports,^(15,17) *BAP1* inactivation caused by deletion of a whole gene or several exons in sporadic MM was rare, but was most frequent in our patients.

In the present study, defective expression of *BAP1* in MM cells with genomic alterations was confirmed by RT-PCR, western blotting, and immunohistochemistry. The possibility of genomic and/or expression changes during cell culture was not completely eliminated. In the case of MM56, from which MM-P cells that were western blot negative were established, some tumor cells of the MM, but not all, exhibited nuclear staining with the same anti-BAP1 antibody. Faint staining by this anti-

body was detected in the cytoplasm of non-tumor mesothelial cells. It should be noted that granular cytoplasmic staining was also seen in some MM tumor specimens having biallelic inactivation of *BAP1*; we are yet to determine the significance of these observations.

It is known that *BAP1* regulates cell proliferation.^(11,14,19,20) The results of the present study suggest that the lack of the tumor suppressor *BAP1* may be more specifically involved in the pathogenesis of epithelioid-type MM rather than non-epithelioid MM. It is tempting to postulate that different pathogenic mechanisms may exert their effects depending on the histological type of MM.

In conclusion, the results of the present study indicate that the loss of *BAP1* expression could be useful in the diagnosis of epithelioid-type MM.

Acknowledgments

This work was supported, in part, by a Grant-in-Aid for Scientific Research (KAKENHI, 20590590). The authors thank Ms Atsuko Iemoto (Hyogo College of Medicine) for technical assistance.

Disclosure Statement

The authors have no conflict of interest.

References

- Selikoff IJ, Hammond EC, Seidman H. Latency of asbestos disease among insulation workers in the United States and Canada. *Cancer* 1980; **46**: 2736–40.
- Nojiri S, Gemba K, Aoe K *et al.* Survival and prognostic factors in malignant pleural mesothelioma: a retrospective study of 314 patients in the west part of Japan. *Jpn J Clin Oncol* 2011; **41**: 32–9.
- Neragi-Miandoab S. Multimodality approach in management of malignant pleural mesothelioma. *Eur J Cardiothorac Surg* 2006; **29**: 14–9.
- Xio S, Li D, Vijg J, Sugarbaker DJ, Corson JM, Fletcher JA. Codelletion of p15 and p16 in primary malignant mesothelioma. *Oncogene* 1995; **11**: 511–55.
- Prins JB, Williamson KA, Kamp MM *et al.* The gene for the cyclin-dependent-kinase-4 inhibitor, *CDKN2A*, is preferentially deleted in malignant mesothelioma. *Int J Cancer* 1998; **75**: 649–53.
- Sekido Y, Pass HI, Bader S *et al.* Neurofibromatosis type 2 (NF2) gene is somatically mutated in mesothelioma but not in lung cancer. *Cancer Res* 1995; **55**: 1227–31.
- Bianchi AB, Mitsunaga SI, Cheng JQ *et al.* High frequency of inactivating mutations in the neurofibromatosis type 2 gene (NF2) in primary malignant mesotheliomas. *Proc Natl Acad Sci USA* 1995; **92**: 10854–8.
- Kratzke RA, Otterson GA, Lincoln CE *et al.* Immunohistochemical analysis of the p16INK4 cyclin-dependent kinase inhibitor in malignant mesothelioma. *J Natl Cancer Inst* 1995; **87**: 1870–5.
- Papp T, Schipper H, Pemsel H *et al.* Mutational analysis of N-ras, p53, p16INK4a, p14ARF and CDK4 genes in primary human malignant mesotheliomas. *Int J Oncol* 2001; **18**: 425–33.
- Yoshikawa Y, Sato A, Tsujimura T *et al.* Frequent deletion of 3p21.1 region carrying semaphorin 3G and aberrant expression of the genes participating in semaphorin signaling in the epithelioid type of malignant mesothelioma cells. *Int J Oncol* 2011; **39**: 1365–74.
- Jensen DE, Proctor M, Marquis ST *et al.* BAP1: a novel ubiquitin hydrolase which binds to the BRCA1 RING finger and enhances BRCA1-mediated cell growth suppression. *Oncogene* 1998; **16**: 1097–112.
- Nishikawa H, Wu W, Koike A *et al.* BRCA1-associated protein 1 interferes with BRCA1/BARD1 RING heterodimer activity. *Cancer Res* 2009; **69**: 111–9.
- Harbour JW, Onken MD, Roberson ED *et al.* Frequent mutation of BAP1 in metastasizing uveal melanomas. *Science* 2010; **330**: 1410–3.
- Ventii KH, Devi NS, Friedrich KL *et al.* BRCA1-associated protein-1 is a tumor suppressor that requires deubiquitinating activity and nuclear localization. *Cancer Res* 2008; **68**: 6953–62.
- Bott M, Brevet M, Taylor BS *et al.* The nuclear deubiquitinase BAP1 is commonly inactivated by somatic mutations and 3p21.1 losses in malignant pleural mesothelioma. *Nat Genet* 2011; **43**: 668–72.
- Wiesner T, Obenaus AC, Murali R *et al.* Germline mutations in BAP1 predispose to melanocytic tumors. *Nat Genet* 2011; **43**: 1018–21.
- Testa JR, Cheung M, Pei J *et al.* Germline BAP1 mutations predispose to malignant mesothelioma. *Nat Genet* 2011; **43**: 1022–5.
- Abdel-Rahman MH, Pilarski R, Cebulla CM *et al.* Germline BAP1 mutation predisposes to uveal melanoma, lung adenocarcinoma, meningioma, and other cancers. *J Med Genet* 2011; **48**: 856–9.
- Machida YJ, Machida Y, Vashisht AA, Wohlschlegel JA, Dutta A. The deubiquitinating enzyme BAP1 regulates cell growth via interaction with HCF-1. *J Biol Chem* 2009; **284**: 34179–88.
- Misaghi S, Ottosen S, Izrael-Tomasevic A *et al.* Association of C-terminal ubiquitin hydrolase BRCA1-associated protein 1 with cell cycle regulator host cell factor 1. *Mol Cell Biol* 2009; **29**: 2181–92.

Supporting Information

Additional Supporting Information may be found in the online version of this article:

Table S1. Characteristics of the cells and tumor specimens used in the present study.

Table S2. Copy number ratio of *BAP1* gene, as determined by CGH array and real-time PCR.

Please note: Wiley-Blackwell are not responsible for the content or functionality of any supporting materials supplied by the authors. Any queries (other than missing material) should be directed to the corresponding author for the article.

Deficiency of Fyn protein is prerequisite for apoptosis induced by Src family kinase inhibitors in human mesothelioma cells

Ryoji Eguchi^{1,2}, Shuji Kubo³, Hiromi Takeda¹,
Toshiro Ohta⁴, Chiharu Tabata², Hiroyasu Ogawa¹,
Takashi Nakano² and Yoshihiro Fujimori^{1,*}

¹Laboratory of Cell Transplantation, Institute for Advanced Medical Sciences, ²Department of Thoracic Oncology and ³Department of Genetics, Hyogo College of Medicine, Nishinomiya, Hyogo 663-8501, Japan and ⁴Department of Food and Nutritional Sciences, Graduate School of Nutritional and Environmental Sciences, University of Shizuoka, Shizuoka 422-8526, Japan

*To whom correspondence should be addressed. Tel/Fax: +81 798 45 6599; Email: fuji-y@hyo-med.ac.jp

Malignant mesothelioma is an aggressive tumor arising from mesothelial cells of serous membranes. Src family kinases (SFKs) have a pivotal role in cell adhesion, proliferation, survival and apoptosis. Here, we examined the effect of SFK inhibitors in NCI-H2052, ACC-MESO-4 and NCI-H28 cells, mesothelioma cell lines and Met5A, a human non-malignant mesothelial cell line. We found that PP2, a selective SFK inhibitor, inhibited SFK activity and induced apoptosis mediated by caspase-8 in NCI-H28 but not Met5A, NCI-H2052 and ACC-MESO-4 cells. Src, Yes, Fyn and Lyn protein, which are members of the SFK, were expressed in these cell lines, whereas NCI-H28 cells were deficient in Fyn protein. Small interfering RNA (siRNA) targeting Fyn facilitated PP2-induced apoptosis mediated by caspase-8 in NCI-H2052 and ACC-MESO-4 cells. PP2 reduced Lyn protein levels and suppressed SFK activity in all mesothelioma cell lines. Lyn siRNA induced caspase-8 activation and apoptosis in NCI-H28 cells but not in NCI-H2052 and ACC-MESO-4 cells. However, double RNA interference knockdown of Fyn and Lyn induced apoptosis accompanied by caspase-8 activation in NCI-H2052 and ACC-MESO-4 cells. Dasatinib, an inhibitor of multi-tyrosine kinases including SFK, also inhibited SFK activity and induced reduction of Lyn protein levels, caspase-8 activation and apoptosis in NCI-H28 cells but not in other cell lines. Present study suggests that SFK inhibitors induce caspase-8-dependent apoptosis caused by reduction of Lyn protein in Fyn-deficient mesothelioma cells.

Introduction

Malignant mesothelioma is an aggressive tumor arising from mesothelial cells of serous membranes, including pleura, peritoneum and pericardium (1–3). Mesothelioma is highly resistant to most chemotherapeutic agents (3), and radiation and surgical therapy generally show limited efficacy (3–5). New approaches for the treatment of malignant mesothelioma are urgently required.

Src family kinases (SFKs) are non-receptor and cytoplasmic tyrosine kinases that have a critical role in cell adhesion, proliferation, survival and apoptosis. In SFKs, Src, Yes and Fyn show ubiquitous expression, whereas others, including Lyn, exhibit more restricted tissue localization (6,7). SFK binds to focal adhesion kinase (FAK), a widely expressed cytoplasmic protein tyrosine kinase. Within SFK–FAK complex, SFK can trans-phosphorylate Tyr-576 and Tyr-577 in the kinase domain of FAK, which regulates migration, cell spreading and focal contact during cell motility (8,9).

In response to apoptotic stimuli, caspases relay messages through so-called initiator caspases to effector caspases (10). Dephosphorylation of Tyr-380, Tyr-397 and Tyr-465 in caspase-8, an initiator caspase, results

in caspase-8 activation (11,12). Caspase cascade mediates apoptotic processes, such as externalization of phosphatidylserine, followed by cell death (10).

To explore a new therapeutic target against mesothelioma, we investigated the effects of SFK inhibitors, PP2 and dasatinib, on human mesothelioma cell lines, NCI-H2052, ACC-MESO-4 and NCI-H28 cells and a human non-malignant mesothelial cell line, Met5A. We found that SFK inhibitors induced apoptosis in NCI-H28 cells, which were deficient in Fyn protein. Further clarification of cell signaling pathways revealed that deficiency of Fyn protein is prerequisite for apoptosis induced by SFK inhibitors in human mesothelioma cells.

Materials and methods

Cell lines and culture

A non-malignant transformed human pleural mesothelial cell line, Met5A and two human mesothelioma cell lines, NCI-H2052 and NCI-H28, were obtained from the American Type Culture Collection (Rockville, MD). Another human mesothelioma cell line, ACC-MESO-4, was purchased from the RIKEN Bio-Research Center (Tsukuba, Japan). Cells were cultured as monolayers in RPMI-1640 medium (Sigma, St Louis, MO) with 10% fetal bovine serum (Sigma) at 37°C under a humidified atmosphere containing 5% CO₂.

Reagents and inhibitors

Antitumor agents and inhibitors were prepared in dimethyl sulfoxide using the following stock solutions: 10 mM PP2, 20 mM zIE(OMe)TD(OMe)-fmk, 40 mM zVAD(OMe)-fmk (BIOMOL, Plymouth Meeting, PA), 25 mM MG132 (BIOMOL) and 5 mM dasatinib (Biovision, Mountain View, CA). Dimethyl sulfoxide was used as a vehicle control as appropriate. All other chemicals were purchased from Sigma.

Treatment with antitumor agents and inhibitors

Cells were seeded as described below and cultured for 24 h. Old medium was aspirated, and fresh medium containing PP2 or dasatinib was added. For PP2 treatment, zVAD, MG132 or vehicle (dimethyl sulfoxide) was added to fresh medium containing PP2. Cells were then cultured for 3–72 h.

Cell viability analysis

Cells were seeded in a 96-well plate (Becton Dickinson Labware, Franklin Lakes, NJ) at 2×10^3 cells per well. Cell proliferation was determined by a colorimetric assay using Cell Counting Kit-8 (Dojin Chemical Institute, Kumamoto, Japan) according to the manufacturer's protocol. Color intensity was quantified as described earlier (13).

Western blotting and antibodies

Western blotting was performed as described earlier (13). Antibodies used to detect phospho-Src family (Tyr-416, #2101), phospho-FAK (Tyr-576/577, #3281), full-length and cleaved caspase-8 (#9746), caspase-3 (#9662), cleaved caspase-3 (#9661), Src (#2108) and phospho-Lyn (Tyr-507, #2731) were purchased from Cell Signaling Technology (Beverly, MA). Glyceraldehyde-3-phosphate dehydrogenase (GAPDH) antibody (#FL-335) was obtained from Santa Cruz Biotechnology (Santa Cruz, CA). FAK (#610087), Yes (#610375), Fyn (#610163) and Lyn antibody (#610003) were purchased from BD Biosciences (San Jose, CA). All western blot analyses were performed three times and the representative data are shown.

Flow cytometric analysis of apoptosis

Apoptosis was analyzed by flow cytometry using an Annexin V (Ax)-fluorescein isothiocyanate Kit (Medical & Biological Laboratories Co. Ltd, Nagoya, Japan) as described earlier (13). Briefly, 1×10^5 cells in a 60 mm dish (Becton Dickinson Labware) treated with PP2 or dasatinib were trypsinized, washed with phosphate-buffered saline and then labeled with Ax-fluorescein isothiocyanate and propidium iodide. Fluorescence intensity was measured using a Cytomics FC 500 flow cytometer and CXP software (Beckman Coulter, Fullerton, CA).

Quantitative reverse transcription-PCR analysis

Total RNA was isolated from cells using TRIzol reagent (Enzo Life Sciences, Farmingdale, NY). First-strand complementary DNA was synthesized from the

Abbreviations: FAK, focal adhesion kinase; GAPDH, glyceraldehyde-3-phosphate dehydrogenase; mRNA, messenger RNA; RNAi, RNA interference; SFK, Src family kinase; siRNA, small interfering RNA.

total RNA (1.25 µg) using the PrimeScript RT reagent kit (Takara Bio, Ohtsu, Japan) according to the manufacturer's instructions. PCR was performed on the synthesized complementary DNA product using TaqMan Gene Expression Master Mix (Applied Biosystems, Foster City, CA) according to the manufacturer's protocol. All reactions were carried out in triplicate. The sequences of the PCR primer pairs and fluorogenic probes used for Fyn and GAPDH are available on the Applied Biosystems website (<http://www.appliedbiosystems.com/absite/us/en/home.html>); Fyn assay ID: Hs00176628_m1; GAPDH assay ID: Hs99999905_m1). The amplification conditions were as follows: denaturation at 95°C for 15 s and annealing/extension at 60°C for 1 min for 60 cycles. The PCR products were analyzed using the ABI 7500 real-time PCR system (Applied Biosystems). Each messenger RNA (mRNA) level was normalized to the corresponding GAPDH mRNA level used as an internal control.

RNA interference

Small interfering RNAs (siRNAs) targeting Fyn [FYN Stealth Select RNA interference (RNAi) HSS103882], Yes (YES Stealth Select RNAi HSS187723) and Lyn (LYN Stealth Select RNAi HSS106213) and Stealth RNAi Negative Control Duplexes were purchased from Invitrogen (Carlsbad, CA). As control siRNA, #12935-146 (#146), #12935-115 (#115) and #12935-147 were used in NCI-H2052, ACC-MESO-4 and NCI-H28 cells, respectively. Stealth siRNA duplex oligoribonucleotides against Src (GenBank™ accession number NM_005417) were synthesized by Invitrogen. The sequences were as follows: sense 5'-CUGUGUUGACAAUCUGGAGCCG-3' and antisense 5'-CGGCUCAGAUUGUCAACAACACAG-3'. The duplex oligoribonucleotides were dissolved in diethyl pyrocarbonate-treated water to make a 20 µM. Transient transfection of siRNAs was carried out using Lipofectamine RNAiMAX (Invitrogen) according to the manufacturer's instructions. Stealth RNAi compounds were used at a concentration of 10 nM in transfections as described earlier (13). Briefly, 2 × 10⁵ cells were incubated in 10 ml of

RPMI-1640 medium in a 100 mm dish overnight. Lipofectamine RNAiMAX and siRNA were each dissolved in 1 ml RPMI-1640 medium for 5 min at room temperature, combined and incubated for 15 min at room temperature to form complexes. Two milliliters of the mixture was added to the cell culture and incubated for 48 h. The cells were harvested by trypsinization and were seeded in a dish for PP2 treatment as described above.

Statistical analysis

All data are presented as the mean ± standard error of three independent experiments. Comparisons between two groups were performed using Student's unpaired *t*-test (**P* < 0.05, ***P* < 0.01 and ****P* < 0.005).

Results

PP2 induces apoptosis mediated by caspase-8 in NCI-H28 cells

We analyzed the effects of PP2, a selective SFK inhibitor, on mesothelioma cell lines (Figure 1). PP2 suppressed cell viability of all mesothelioma cell lines used more markedly than that of Met5A cells in a concentration-dependent manner (Figure 1A). We used an antibody recognizing phosphorylation of tyrosine residue corresponding to Tyr-416 of Src in various SFKs (Figure 1B). PP2 inhibited the phosphorylation of SFK (lower two arrows in Figure 1B) and that of p-FAK in a concentration-dependent manner in all mesothelioma cell lines used. These results show that enzyme activity of SFK is suppressed by PP2. Intriguingly, PP2 significantly induced apoptosis in NCI-H28 cells (Figure 1C). In NCI-H28 cells, PP2 also induced cleavage of caspase-8 and caspase-3 in a time-dependent manner (Figure 1D). Furthermore, PP2-induced apoptosis in NCI-H28 cells

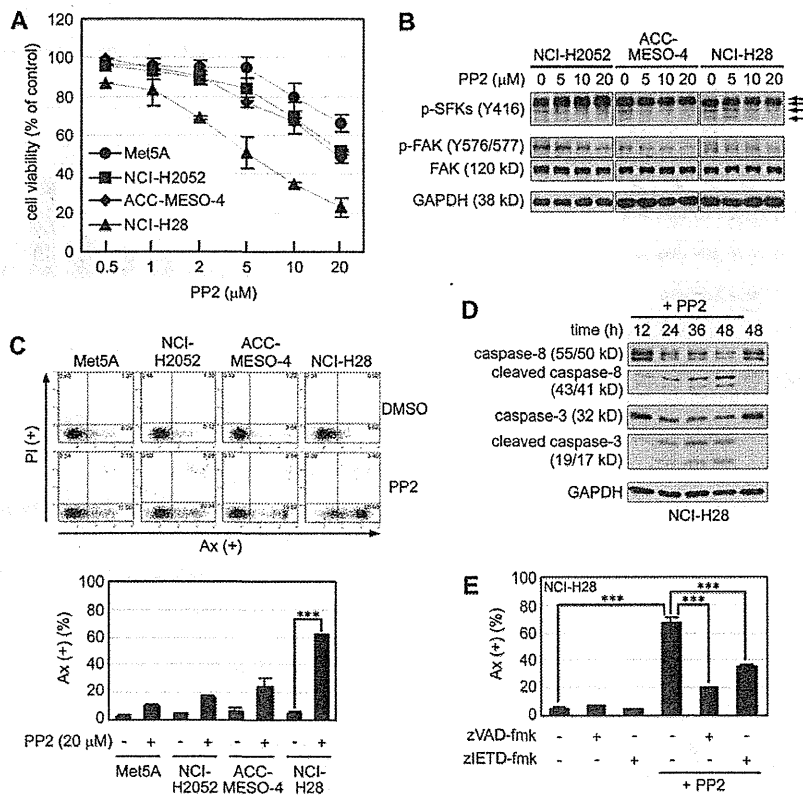


Fig. 1. PP2 induces apoptosis mediated by caspase-8 in NCI-H28 cells. (A) PP2 suppresses cell viability of NCI-H2052, ACC-MESO-4 and NCI-H28 cells more markedly than that of Met5A cells. These cell lines were treated with PP2 for 48 h at the indicated concentrations. Cell viability was assessed using the Cell Counting Kit-8 assay. (B) PP2 suppresses enzyme activity of SFK. Cell extracts were prepared from NCI-H2052, ACC-MESO-4 and NCI-H28 cells treated with 5–20 µM PP2 for 6 h as described in Materials and methods. Arrows indicate phosphorylation of Tyr-416 in various SFKs. (C) PP2 induces apoptosis in NCI-H28 cells, but not in Met5A, NCI-H2052 and ACC-MESO-4 cells. The numbers of (Ax+) apoptotic cells were markedly increased 72 h after the treatment with 20 µM PP2 in NCI-H28 cells but not in other cell lines. (D) PP2 induces activation of caspase-8 and caspase-3. Cell extracts were prepared from NCI-H28 cells treated with 20 µM PP2 for 12–48 h. (E) PP2-induced apoptosis in NCI-H28 cells is suppressed by zVAD-fmk and zIETD-fmk. NCI-H28 cells were treated with 20 µM PP2 alone or together with 100 µM zVAD-fmk and 50 µM zIETD-fmk for 72 h and analyzed for Ax(+) apoptotic cells by flow cytometry.

was significantly suppressed by zVAD-fmk, a broad-spectrum caspase inhibitor, and zIETD-fmk, a specific caspase-8 inhibitor (Figure 1E). These results suggest that PP2 suppresses SFK activity and induces apoptosis mediated by caspase-8 in NCI-H28 cells.

Deficiency of Fyn protein is caused by transcriptional repression of Fyn mRNA in NCI-H28 cells, and Lyn is expressed in mesothelial and mesothelioma cells

We examined whether SFK expression is involved in PP2-induced apoptosis in mesothelioma cells (Figure 2). Src, Yes and Lyn protein were detected in all cell lines used, but NCI-H28 cells were deficient in Fyn protein, whereas it was expressed in other three cell lines (Figure 2A). Phosphorylation of SFK in NCI-H2052 and ACC-MESO-4 but not NCI-H28 cells was higher than that in Met5A cells. We then examined expression of Fyn mRNA using quantitative reverse transcription-PCR (Figure 2B). It was found that Fyn mRNA expression in NCI-H28 cells was much lower than that in other cell lines used. Additional experiments using other PCR primer pairs and fluorogenic probes also showed that Fyn mRNA was not completely absent in NCI-H28 cells (data not shown). These results suggest that deficiency of Fyn protein is caused by transcriptional repression of Fyn mRNA in NCI-H28 cells and that Lyn is expressed in mesothelial and mesothelioma cells.

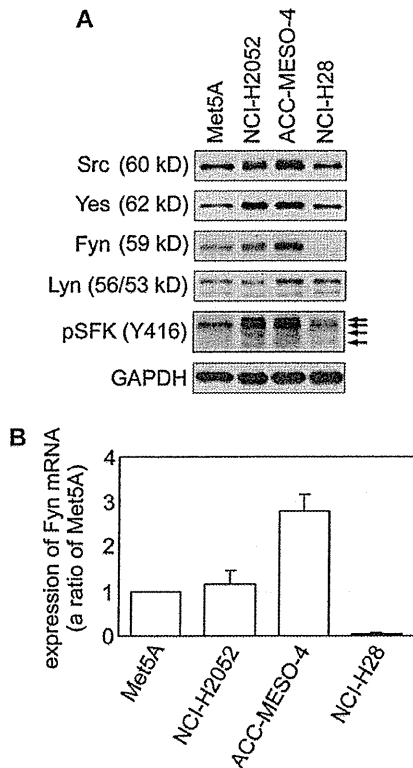


Fig. 2. Deficiency of Fyn protein is caused by transcriptional repression of Fyn mRNA in NCI-H28 cells. (A) Expression and phosphorylation of SFK in Met5A, NCI-H2052 and ACC-MESO-4 and NCI-H28 cells. Cell extracts were prepared from these cell lines incubated for 72 h. (B) Fyn synthesis is suppressed by transcriptional repression of Fyn mRNA in NCI-H28 cells. Total RNA was isolated from these cells after incubation for 72 h as described in Materials and methods.

Fyn-knockdown facilitates PP2-induced apoptosis in mesothelioma cells

To further investigate whether transcriptional repression of Fyn mRNA is related to PP2-induced apoptosis, we performed RNAi using siRNA targeting Fyn in NCI-H2052 and ACC-MESO-4 cells (Figure 3). Fyn siRNA abrogated expression of Fyn protein with no effect on expression of Src, Yes and Lyn protein (Figure 3A). In NCI-H2052 and ACC-MESO-4 cells treated with Fyn siRNA, PP2 induced apoptosis more significantly than in these cells treated with control siRNA (Figure 3B). Furthermore, PP2 induced cleavage of caspase-8 and caspase-3 in these Fyn-knockdown mesothelioma cell lines (Figure 3C). These results suggest that Fyn-knockdown facilitates PP2-induced apoptosis in Fyn-expressing mesothelioma cells.

SFK inhibition induces apoptosis in Fyn-deficient mesothelioma cells

We then analyzed whether PP2-induced apoptosis is related to SFK inhibition in NCI-H28 cells (Figure 4). Western blot analysis showed that PP2 suppressed phosphorylation of Tyr-416 in SFKs and that of

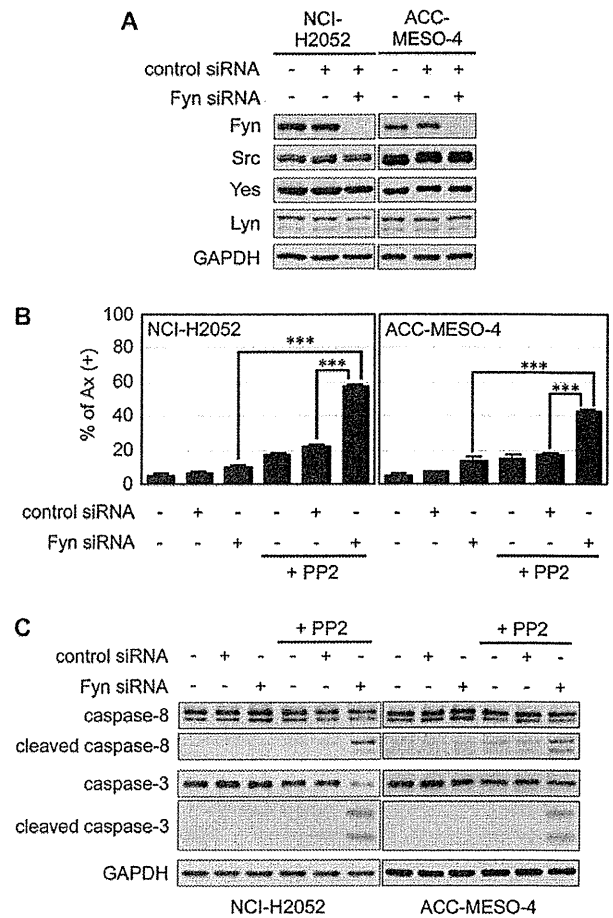


Fig. 3. Fyn-knockdown facilitates PP2-induced apoptosis in mesothelioma cells. (A) Fyn-knockdown in mesothelioma cells. NCI-H2052 and ACC-MESO-4 cells were transfected with 10 nM siRNA against Fyn mRNA or 10 nM control siRNA for 48 h, harvested by trypsinization and incubated for 24 h. Cell extracts were prepared from NCI-H2052 and ACC-MESO-4 cells after the incubation for 24 h. (B) Fyn-knockdown facilitates PP2-induced apoptosis in mesothelioma cells. NCI-H2052 and ACC-MESO-4 cells, transfected with Fyn and control siRNAs, were treated with 20 μM PP2 for 72 h and analyzed for Ax (+) apoptotic cells by flow cytometry. (C) PP2 induces activation of caspase-8 and caspase-3 in Fyn-knockdown mesothelioma cells. NCI-H2052 and ACC-MESO-4 cells, transfected with Fyn and control siRNA, were treated with 20 μM PP2 for 48 h.